UNIVERSITÀ DEGLI STUDI DI BOLOGNA – ALMA MATER STUDIORUM

Dipartimento di Colture Arboree

Dottorato di Ricerca (XIX ciclo) in:
Colture arboree ed agrosistemi forestali ornamentali e paesaggistici

Settore disciplinare:
AGR/05 – Assestamento Forestale e Selvicoltura

ROLE OF XANTHOPHYLL AND WATER-WATER CYCLES IN THE PROTECTION OF PHOTOSYNTHETIC APPARATUS IN *Arbutus unedo* AND *Arabidopsis thaliana*

Dissertazione presentata dal Dott. Alessandro Zamboni

Tutore:
Prof. Federico Magnani

Coordinatore:
Prof. Silviero Sansavini

Co - tutore:
Dr. Giustino Tonon

Anno 2007

Role of xanthophyll and water-water cycles in the protection of photosynthetic apparatus in *Arbutus unedo* and *Arabidopsis thaliana*

Index

Abstract

Photosynthetic organisms have sought out the delicate balance between efficient light harvesting under limited irradiance and regulated energy dissipation under excess irradiance. One of the protective mechanisms is the thermal energy dissipation through the xanthophyll cycle that may transform harmlessly the excitation energy into heat and thereby prevent the formation of damaging active oxygen species (AOS). Violaxanthin de-epoxidase (VDE) converts violaxanthin (V) to antheraxanthin (A) and zeaxanthin (Z) defending the photosynthetic apparatus from excess of light.

Another important biological pathway is the chloroplast water-water cycle, which is referred to the electrons from water generated in PSII reducing atmospheric O_2 to water in PSI. This mechanism is active in the scavenging of AOS, when electron transport is slowed down by the over-reduction of NADPH pool.

The control of the VDE gene and the variations of a set of physiological parameters, such as chlorophyll florescence and AOS content, have been investigated in response to excess of light and drought condition using *Arabidopsis thaliana* and *Arbutus unedo*.. Pigment analysis showed an unambiguous relationship between xanthophyll de-epoxidation state ((A+Z)/(V+A+Z)) and VDE mRNA amount in not-irrigated plants. Unexpectedly, gene expression is higher during the night when xanthophylls are mostly epoxidated and VDE activity is supposed to be very low than during the day.

The importance of the water-water cycle in protecting the chloroplasts from light stress has been examined through *Arabidopsis* plant with a suppressed expression of the key enzyme of the cycle: the thylakoid-attached copper/zinc superoxide dismutase. The analysis revealed changes in transcript expression during leaf development consistent with a signalling role of AOS in plant defence responses but no difference was found any in

photosynthesis efficiency or in AOS concentration after short-term exposure to excess of light.

Environmental stresses such as drought may render previously optimal light levels excessive. In these circumstances the intrinsic regulations of photosynthetic electron transport like xanthophyll and water-water cycles might modify metabolism and gene expression in order to deal with increasing AOS.

1. Introduction

Plants are subjected to several harsh environmental stresses that adversely affect growth, metabolism and yield. Drought, salinity, low and high temperatures, flood, pollutants and radiation are the stress factors limiting the productivity of the ecosystems.(Reddy, Chaitanya, & Vivekanandan 2004).

Even under optimal condition many metabolic processes produce active oxygen species (AOS). In plants, the most important of these are driven by or associated with light dependent events (Foyer, Lelandais, & Kunert 1994). AOS, resulting from excitation or incomplete reduction of molecular oxygen, are unwelcome harmful by-products of normal cellular metabolism in aerobic organisms. Plants, facing a burden of excess AOS, initially developed various protective mechanisms, such as small antioxidant molecules and antioxidant enzymes, to keep AOS level under control (Apel & Hirt 2004). As these protective mechanisms were robust, plants evolved an elaborate network of AOS-producing and detoxifying enzymes (represented by at least 289 genes in *Arabidopsis*) to adjust AOS levels according to the cellular needs in different cell types and organs at a particular time and at different developmental stages. This evolutionary advance permitted AOS to be co-opted as signalling molecules that control cell proliferation and cell death to regulate plant growth and development, adaptation to abiotic stress factors and proper responses to pathogen attack (Apel & Hirt 2004). To influence all those processes in a range of tissues at

different developmental stages, the biological response to the altered AOS levels requires remarkable specificity. This specificity is ensured by multiple interacting factors, including the chemical identity of AOS, intensity of the signal, site of AOS production, developmental stage of the plant and previous stress encountered (Apel & Hirt 2004;Gechev et al. 2006).

Under non stressful condition, the antioxidative defence system provides adequate protection against AOS, but plants in their natural environments are very often exposed to sudden increase in light intensity, which results in the absorption of excitation energy in excess of that required for metabolism. High irradiation causes a potentially destructive excess of light energy that is absorbed by the chlorophylls, in this condition the control of the increase in AOS production is essential to avoid the oxidative stress leading to photoinhibition and eventually to cell death (Foyer et al. 1994;Mullineaux, Karpinski, & Baker 2006;Reddy, Chaitanya, & Vivekanandan 2004).

The photosynthetic electron transport system is the major source of AOS, having potential to generate singlet oxygen ($^1O_2$) and superoxide ($O_2^{-\bullet}$). The production of these unstable molecules is an unavoidable consequence of the operation of the photosynthetic electron transport chain in an oxygen atmosphere (Arora, Sairam, & Srivastava 2002) but become significantly higher and dangerous for the cell under stressful conditions.

Light is captured by a set of light-harvesting complexes (LHCs) that funnel light energy into photochemical reaction centres, photosystem (PS) I and PSII. Special subset of chlorophylls molecules in these photosystems are excited by light energy, allowing electrons on them to be transferred through a series of redox carriers called the electron transfer chain (ETC), beginning with the oxygen evolving complex (OEC) of PSII through the plastoquinone (PQ) pool, the cytochrome b_6f complex and plastocyanin, and finally through PSI. Electrons from PSI are transferred to ferredoxin which, in turn, reduces $NADP^+$ to NADPH via ferredoxin:$NADP^+$ oxidoreductase. This linear electron flux (LEF) to $NADP^+$ is coupled to proton release at the

OEC, and 'shuttling' of protons across the thylakoid membrane by the PQ pool and the Q-cycle at the cyt b_6f complex, which establish a proton

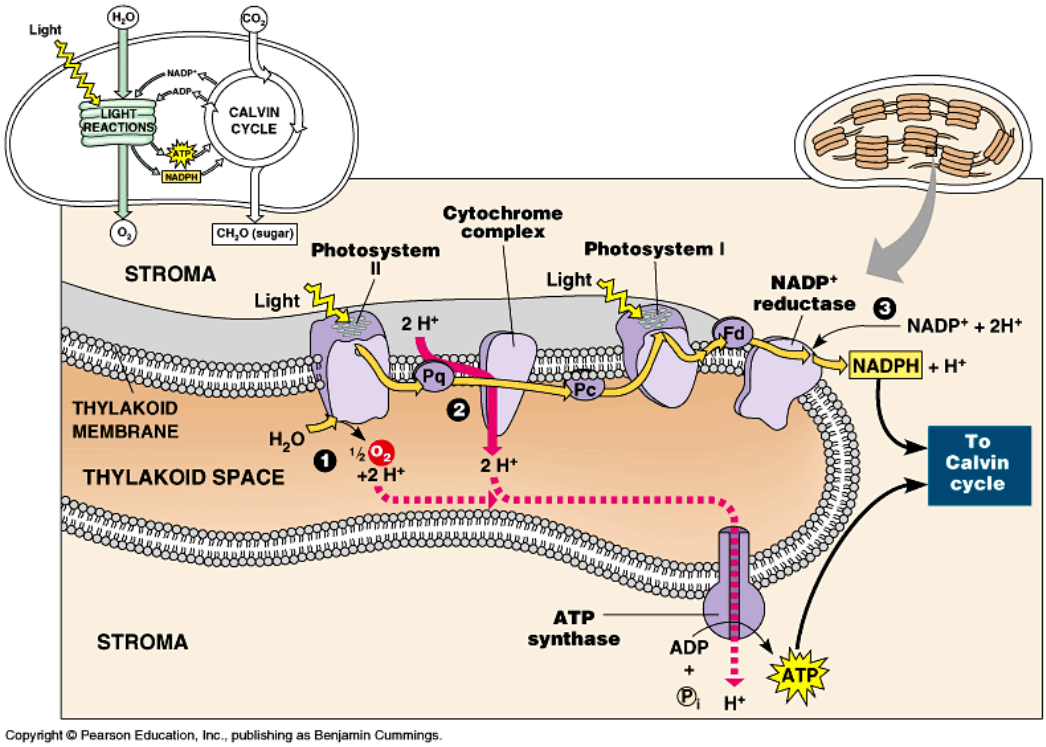

Fig. 1 Diagram of the photosynthetic electron transport system. 1. Oxygen evolving complex produces $2H^+$ from each water molecule processed. 2. Cytochrome b_6f compex pumps H^+ into the lumen thanks to the Q-cycle. 3. $NADP^+$ reductase consumes H^+ generating NADPH. The processes 1, 2 and 3 lead to an increment in ΔpH between lumen and stroma.

motive force (*pmf*) that drives the synthesis of ATP by chemiosmotic coupling through the chloroplast ATP synthase (Fig.1).

In general, over-excitation of PSII is prevented largely by antenna down-regulation, which dissipates excess excitation energy as heat. This involves a series of processes, which are collectively termed non-photochemical quenching (NPQ) and typically measured by the quenching of chlorophyll-a fluorescence (Cruz et al. 2005;Maxwell & Johnson 2000). This 'quenching' of light energy in the antenna is dependent on the 'energization' of the thylakoid membrane and involves at least two processes: the xanthophyll cycle, and protonation of amino acid side-chains on an antenna associated chlorophyll binding protein, PsbS.

Limiting the quantity of energy available in the reaction centres could be not sufficient since, even under stressful conditions, maintaining an electron flow through the photosynthetic membrane is vital for preventing damage to plant cells.

Two different pathways that are thought to cooperate in protecting the photosynthetic apparatus from photo-oxidative stress, sustaining electron transfer, are the cyclic electron flow and the water-water cycle (WWC). These pathways shunt electrons through the photosynthetic apparatus and maintain the pH gradient in the chloroplast, which is essential for the function of many biological processes first the zeaxanthin cycle.

1.1 Thermal energy dissipation

Incident light can vary on seasonal base or rapidly due to passing clouds or sunflecks within the same day. With increasing light intensity, photosynthetic utilisation of absorbed light energy reaches saturation, while light absorption continues to increase. This can result in a mismatch between excitation of photosynthetic pigments and plant ability to use the excitation energy for photosynthesis (Baroli et al. 2004;Demmig et al. 1987).

One of the ways in which this balancing act is accomplished is through the regulation of photosynthetic light harvesting. On a time scale of seconds to minutes, non-photochemical quenching (NPQ) processes in PSII can be induced or disengaged in response to changes in light intensity. The term NPQ reflects the way in which these processes are routinely assayed through measurements of chlorophyll fluorescence (Maxwell & Johnson 2000). Under most circumstances, the major component of NPQ is due to a regulatory mechanism, called qE, which results in the thermal dissipation of excess absorbed light energy in the light-harvesting antenna of PSII. The qE is induced by a low thylakoid lumen pH (i.e. a high ΔpH) that is generated by photosynthetic electron transport in excess light, so it can be considered as a type of feedback regulation of the light-dependent reactions of

photosynthesis. The low thylakoid lumen pH that induces qE has two roles. One role is the pH-dependent activation of a lumen-localized violaxanthin de-epoxidase (VDE) enzyme that catalyses the conversion of violaxanthin to zeaxanthin via the intermediate antheraxanthin (Demmig et al. 1987).

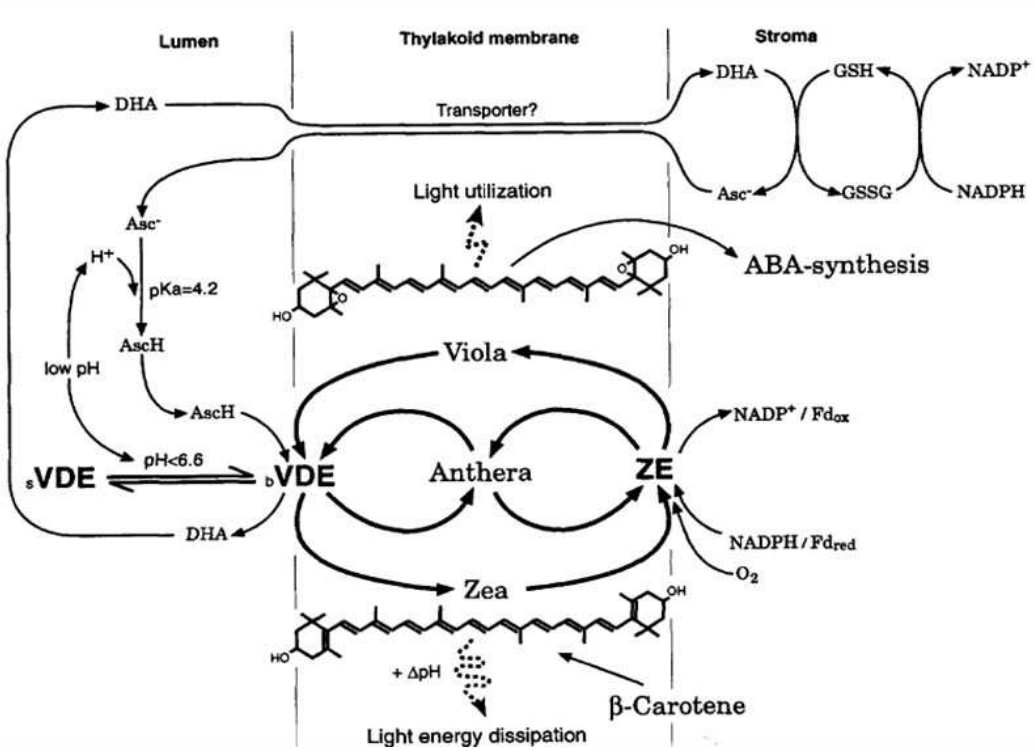

Fig. 2 Model of the regulation of the xanthophyll cycle and its relation to ABA synthesis. sVDE, soluble VDE; bVDE, bound VDE; DHA, dehydroascorbate; Asc^-, ascorbate; AscH, ascorbic acid; GSH, glutathione; Viola, violaxanthin; Anthera, antheraxanthin; Zea, zeaxanthin; Fd, ferredoxin. (Eskling, Arvidsson, & Åkerlund 1997)

The second role of low thylakoid lumen pH is to drive protonation of one or more PSII proteins that are involved in qE (Horton & Ruban 2005). It has been hypothesized that protonation activates a binding site for zeaxanthin in one of the proteins (Gilmore 1997) and as a result an absorbance change (ΔA_{535}) is detectable in leaves and isolated thylakoids, which might be due to a change in the absorption spectrum of zeaxanthin. This alteration of the properties of one or a few zeaxanthin molecules per PSII might allow zeaxanthin to facilitate directly the de-excitation of singlet excited chlorophyll via energy or electron transfer (Holt, Fleming, & Niyogi 2004). Plants that experience light stress in their environment (i.e. sun plants) generally have higher qE capacities and larger xanthophyll pool sizes (sum

of violaxanthin, antheraxanthin and zeaxanthin) than plants growing in shaded environments. Furthermore, mutants that lack qE are sensitive to light stress and have decreased ecological fitness in fluctuating light environments (Demmig-Adams & Adams 2006).

In addition to a low lumen pH and the presence of de-epoxidized xanthophylls like zeaxanthin, qE requires the protein PsbS. This 22 kDa protein was discovered more than 20 years ago in isolated PSII preparations (Berthold, Babcock, & Yocum 1981), but its exact location within PSII is still unknown.

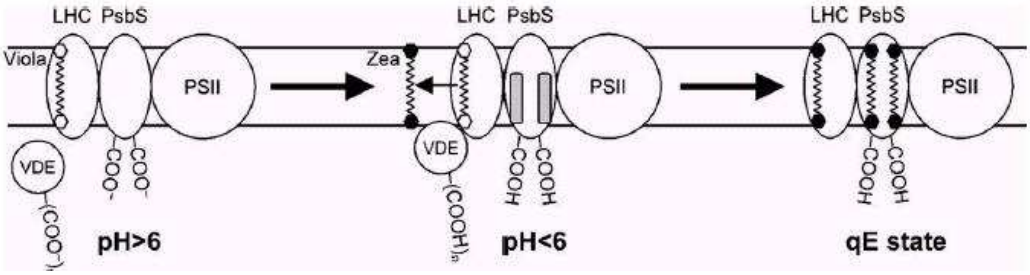

Fig. 3 Schematic model for qE in plants. (Left) In limiting light, the steady-state thylakoid lumen pH is greater than 6. Violaxanthin (Viola) is bound mainly to the V1 site in LHCII and the L2 site in other LHC proteins (such as CP29 and CP26). For simplicity, other pigments (chlorophylls and other carotenoids) are not shown, and only one Viola and one LHC protein are shown per PSII. The various components are not drawn to scale. (Middle) In excess light, the thylakoid lumen pH drops below 6, driving protonation of carboxylate side chains in VDE and PsbS. Protonation of VDE activates the enzyme and allows for its association with the membrane, where it converts multiple Viola molecules to zeaxanthin (Zea). Protonation of glutamate residues E122 and E226 in PsbS activates symmetrical binding sites for xanthophylls with a de-epoxidized b-ring endgroup (i.e. zeaxanthin). (Right) Zea binding to protonated sites in PsbS results in the qE state in which singlet chlorophyll de-excitation is facilitated. Other Zea molecules bind to sites in LHCII and other LHC proteins (Niyogi et al. 2005).

It is likely that PsbS is located between the PSII reaction centre core and the peripheral LHCII, with the functional association possibly occurring between PsbS and the PSII core antenna (Fig.3). The discovery that PsbS is necessary for qE was an important breakthrough in the study of qE, but the mechanism of qE remains one of the last major unresolved mysteries in photosynthesis (Niyogi et al. 2005).

The amount of the PsbS protein in thylakoids is a determinant of qE capacity (Hieber, Kawabata, & YAMAMOTO 2004;Li et al. 2000), and

two lumen-facing glutamate residues in PsbS have been identified as proton-binding sites that are probably involved in sensing lumen pH and turning qE on and off (Niyogi et al. 2005). Evidence for zeaxanthin binding by PsbS in vitro has been reported (Aspinall-O'Dea et al. 2002), and ultrafast PsbS-dependent excitation of zeaxanthin following laser excitation of chlorophyll has been demonstrated (Ma et al. 2003). This places strict constraints on the distance between the nearest chlorophyll and the excited zeaxanthin, which is assumed to reside in PsbS, but chlorophyll binding to PsbS remains to be unequivocally demonstrated (Kalituho et al. 2006). It is possible that the coupled chlorophyll might be located on the periphery of PsbS, perhaps at the interface between PsbS and PSII.

All plants apparently employ PsbS/ΔpH-dependent dissipation under moderate stress (i.e. moderate levels of light excess). Yet, differences in the inherent capacity for this flexible dissipation do exist among plant species. Short-lived, fast-growing crops have lower maximal capacities for flexible dissipation than long-lived, slow-growing tropical evergreens.

This is intuitively logical, since fast-growing crops have much higher intrinsic capacities for photosynthesis, and thus utilize a much greater fraction of full sunlight for photosynthesis and growth, than slow-growing species. The same differences in the patterns of flexible dissipation observed between annuals and evergreens have been found for the corresponding acclimatization patterns of the PsbS protein and the maximal levels of zeaxanthin produced quickly under excess light (Demmig-Adams et al. 2006).

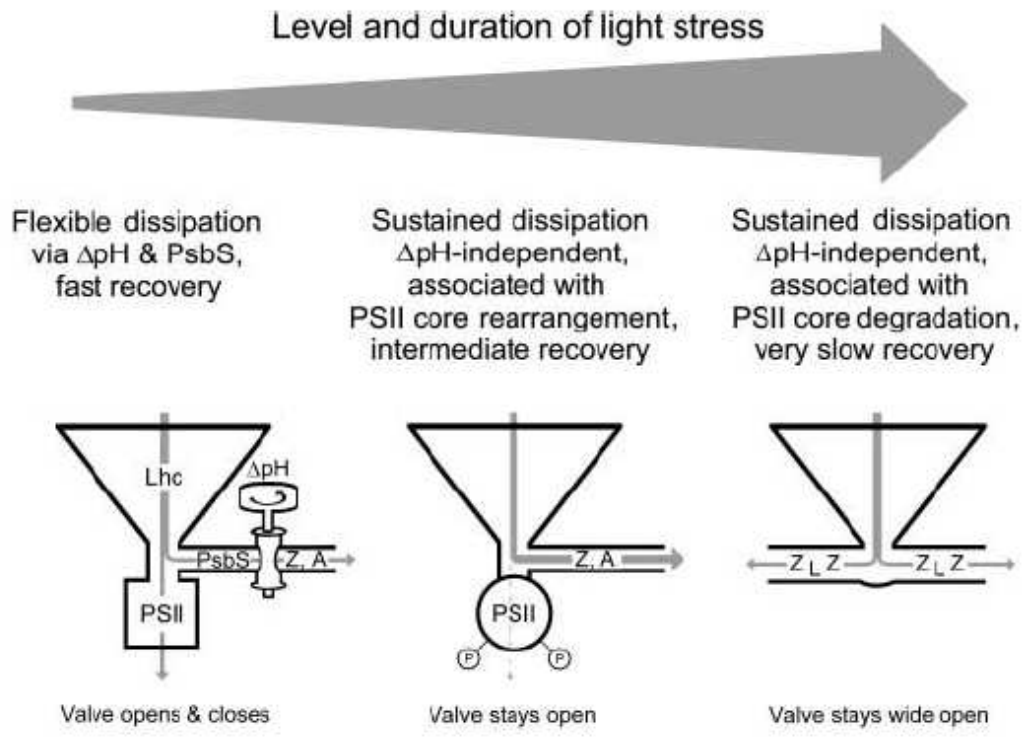

Fig. 4 Scheme showing the relationship between flexible and sustained (trans-thylakoid pH gradient (ΔpH)- independent) forms of energy dissipation with respect to their response to excess light. Lhc, light harvesting complexes; PSII, photosystem II cores in different conformations; P, protein phosphorylation; Z, zeaxanthin; A, antheraxanthin; L, lutein.

Flexible dissipation responds to changes in light environment under favourable conditions as well as to other conditions representing increased levels of excess of excitation as a consequence of decreased ATP utilization. This has been demonstrated for several annual species exposed to limiting levels of soil nitrogen (Logan et al. 1999) or water (Demmig-Adams et al. 2006;Munne-Bosch & Penuelas 2004). However, in many plant species, and evergreens in particular, the most notable change in thermal dissipation under combinations of environmental stress factors is the development of another form of thermal dissipation that is neither ΔpH-dependent nor rapidly reversible.

In addition to the ubiquitous process of flexible dissipation, several forms of sustained dissipation exist (Fig.4). The term ‘sustained’ refers to the fact that this dissipation process does not relax upon darkening of the leaves. A variety of plant species can maintain high levels of NPQ by maintaining an actual ΔpH in darkness at low temperatures (Demmig-Adams et al. 2006).

While this form of thermal dissipation can be sustained for prolonged periods in darkness at low temperatures, it is still ΔpH-dependent and flexible in the sense that warming of leaves will allow this state to be quickly reversed. However, the term ‘sustained’ dissipation is also, and primarily, used in other scenarios where thermal dissipation has different underlying features in fact it is not ΔpH-independent and has truly lost its flexibility.

The difference in the underlying mechanism between flexible and sustained ΔpH-independent dissipation does not appear to be related to zeaxanthin, since this xanthophyll is involved in both types of thermal dissipation as a common factor. Therefore, under lasting stress conditions and in some plant species, the flexible, ΔpH-independent engagement and disengagement of zeaxanthin in dissipation is replaced by a highly effective, but less flexible continuous engagement of zeaxanthin in dissipation, that does not require a ΔpH. Under these latter conditions, the xanthophyll cycle itself is arrested in its photoprotective form – as the photochemical system is maintained in its dissipative state. Sustained, ΔpH-independent photoprotection has been characterized in overwintering evergreens as well as in tropical evergreen species upon transfer from low to high light. Under severe stress, when intrinsic photosynthetic capacity is strongly decreased and PSII core proteins may be degraded, it may be difficult, if not impossible, to generate the pH gradient necessary to convert violaxanthin to zeaxanthin, to protonate PsbS, and engage this ubiquitous dissipation process (Niyogi et al. 2005). At the same time, the need for flexible, rapidly reversible dissipation is also diminished when intrinsic photosynthetic capacity is downregulated and light energy does not need to be quickly rerouted to photosynthesis. The continuous maintenance of the dissipative state can be viewed as an alternative and powerful means of photoprotection under these severe conditions. This unique form of photoprotection may be a prerequisite for the evergreen “lifestyle” (involving persistence throughout entire unfavourable seasons in an inactive state) as opposed to the strategy of short-lived species completing their life cycle during the favourable

season or maintaining growth under moderately unfavourable conditions, but unable to persist under prolonged severe stress.

Sustained, ΔpH-independent dissipation is apparently associated either with a constant rearrangement or with degradation of PSII core proteins (Demmig-Adams et al. 2006;Ebbert et al. 2005). In other words, thermal dissipation may become independent of the actual presence of excess light (and ΔpH) either by a sustained structural change in PSII or the removal of PSII core proteins altogether.

1.2 Water-water cycle

Photosynthesis involves the transfer of electrons from water to NADP+ via two photosystems, the so-called linear path, forming NADPH. Electron transfer also results in proton translocation across the thylakoid membrane, generating a transmembrane pH gradient, which drives the synthesis of ATP. Both NADPH and ATP are then used for carbon fixation. Given that the H+/ATP efficiency of this process is expected to be ~ 4.7, linear electron transport alone is probably unable to generate the ATP/NADPH stoichiometry of 1.5 that is required for carbon fixation, as its maximum H+/NADPH stoichiometry is 6. Alternative electron transport pathways are thus required to provide the “extra” ATP (Breyton et al. 2006). Electron flow to oxygen (the water-water cycle) and cyclic electron flow around PSI were proposed to represent the possible candidates.

Photosynthetic electron transport is characterized by multiplicity of its pathways. Noncyclic electron transport, driven in chloroplast membranes by consecutive operation of two photosystems, is a predominant pathway in most cases. Multiplicity of photosynthetic electron transport pathways signifies that chloroplasts of intact phototrophic cells contain so-called alternative electron transport pathways that operate in addition to noncyclic electron flow and are driven by photoreactions of PSI alone (Egorova & Bukhov 2006). Furthermore, alternative electron flow pathways include several routes. Linear and cyclic flow are not physically separated but,

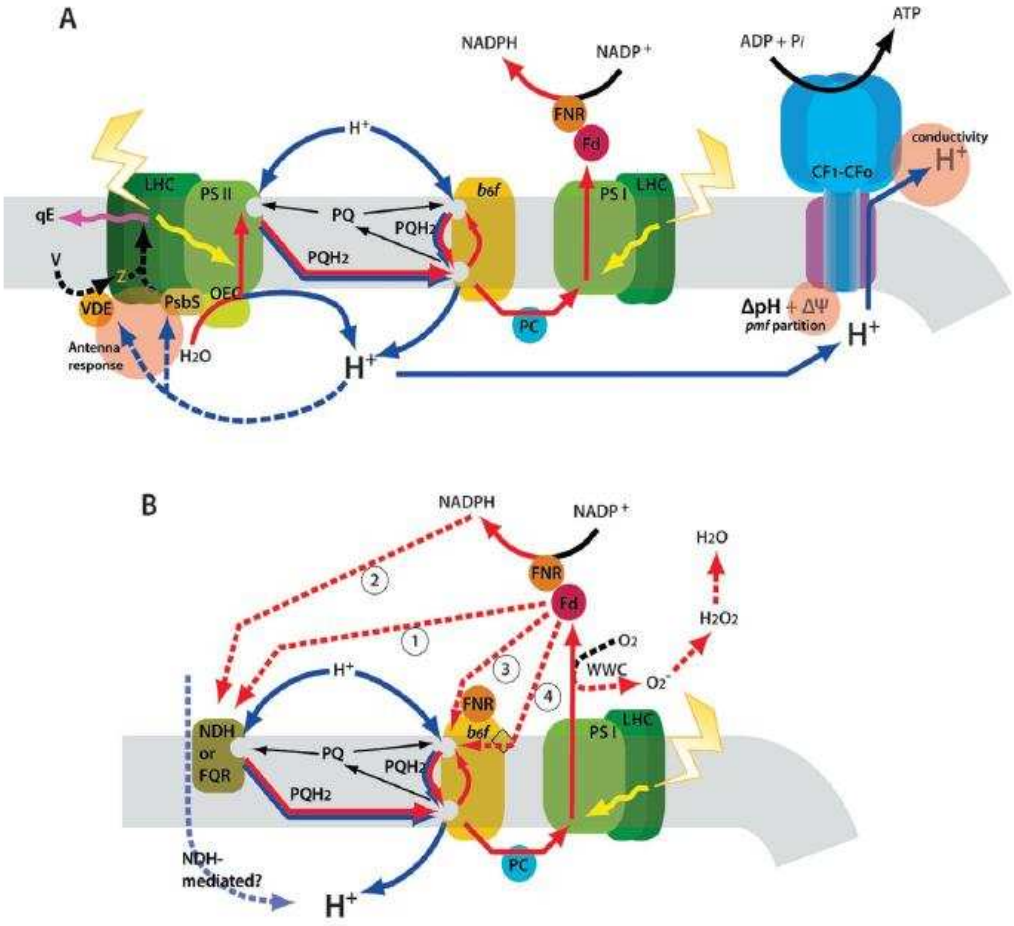

Fig. 5 Primary routes of proton/electron flux and mechanisms of Type I and II flexibility. (A) Energy storage begins with the absorption of light energy (lightning bolts) by light-harvesting complexes (LHC) associated with photosystem (PS) II and I, respectively. Depicted is the linear electron flux (LEF, red arrows) of electrons derived from the oxidation of H_2O at the oxygen evolving complex (OEC) through PSII reducing sequentially plastoquinone (PQ) to a quinol (PQH_2). Bifurcated oxidation of PQH_2 occurs at the cytochrome b6 f complex (b_6f) where half of the electrons are linearly transferred to the $NADP^+$/NADPH couple via plastocyanin (PC), PSI, ferredoxin (Fd), and ferredoxin-$NADP^+$ oxidoreductase (FNR), and the other half of the electrons will return to the PQH_2 pool. Proton flux (blue arrows) originates from H_2O splitting at the OEC and the cyclic reduction and oxidation of PQ/PQH_2, establishing an electrochemical gradient of protons across the thylakoid membrane (pmf), comprised of pH (ΔpH) and electric field (Δw) components. Total pmf drives ATP synthesis from ADP and Pi as protons move down their electrochemical gradient through the CF1-CFO ATP synthase. Energy dissipation by qE (purple arrow) is pH-dependent due to the pH-dependent activity of violaxanthin de-epoxidase (VDE), which sequentially reduces violaxanthin (V) to zeaxanthin (Z), and protonation of PsbS. Type II mechanisms (highlighted in red) involve variability in: (i) the response of the antenna to lumen pH, (ii) the conductive properties of the ATP synthase, and (iii) the relative partitioning of pmf into Δw and ΔpH. Type I mechanisms (B) involve alternate routes of electron transfer at the reducing side of PSI, including the water–water cycle (WWC) and cyclic electron flow around PSI (CEF1). The WWC uses the same electron transfer pathways as normal LEF except at the reducing side of PSI it reduces O_2 to O_2^- which is subsequently detoxified to H_2O. As depicted, four carrier pathways have been proposed for the cycling of electrons from PSI back to the PQ pool (CEF1): (1) a ferredoxin-PQ oxidoreductase (FQR), (2) a NADPH-PQ oxidoreductase (NDH), (3) oxidation of Fd by a FNR/b_6f super-complex, and (4) oxidation of, for example, Fd by a newly discovered haem associated with the stromal side of the b_6f complex (Cruz et al. 2005).

rather, that the two systems are in dynamic competition (Fig.5). Once a reducing equivalent is generated at the reducing side of PSI, its involvement in either linear or cyclic flow is determined at the level of the Fd pool. As the diffusionof this protein is not confined, its oxidation by FNR and the NADP+ pool would lead to linear flow, while interaction with a putative Fd oxidizing site located on the stromal side of cyt b_6f or molecular oxygen would initiate cyclic flow (Breyton et al. 2006) or WWC(Asada 1999), respectively.

Although the WWC does not produce any net reductant, it generates *pmf*, which may serve to drive ATP synthesis or to initiate down-regulation of photosynthesis. An estimate based on a survey of more recent work (Badger et al. 2000) suggests that WWC operates at 10% of LEF of C3 photosynthesis, even under conditions of extreme stress. By contrast, higher flux capacities for WWC have been observed in isolated chloroplasts of C3 plants, suggesting that conditions which favour WWC may not be simple to produce *in vivo*. However, there is evidence for the active engagement of the WWC in conjunction with CEF1 in rice leaves, during photosynthetic induction (Makino, Miyake, & Yokota 2002). It was suggested that the supplemental proton flux was required to generate additional ATP for the initiation of the Calvin– Benson cycle from a dark-adapted state. Furthermore, under-expression of thylakoid-associated Cu/Zn-SOD in *Arabidopsis* suppressed photosynthetic activity and growth, which is consistent with the need for detoxification of O_2^- generated by photosynthesis, even in absence of environmental stress condition (Rizhsky, Liang, & Mittler 2003).

Under photon-excess conditions, WWC could have a more important role because physiological electron acceptors are usually not available to PSI. The proton gradient required for ΔpH-dependent qE can be generated via either the cyclic electron flow around PSI or the linear electron flow through the water-water cycle. The cyclic electron flow appears to operate preferentially when the electron supply from PSII is limited, for example, by down-regulation of PSII or excitation of PSI only by far-red light, in the

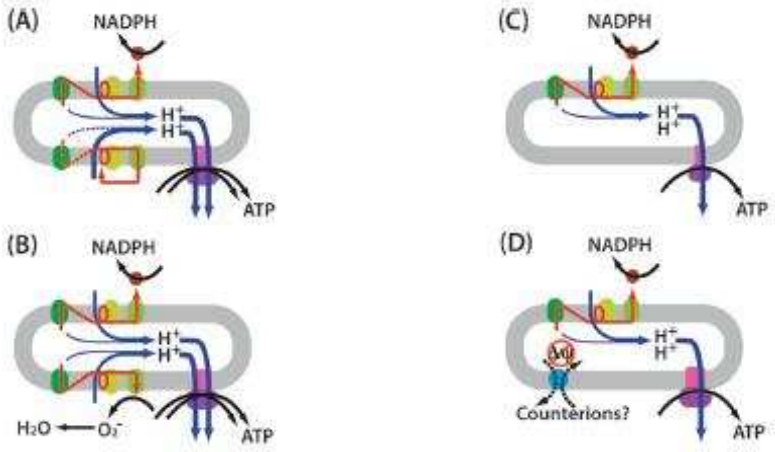

	NADPH	ATP	pmf	ΔpH	qE / LEF
(A) ↑ CEF1	NC	↑	↑	↑	↑
(B) ↑ WWC	NC	↑	↑	↑	↑
(C) ↓ gH^+	NC	NC	↑	↑	↑
(D) ↓ Δψ/pmf	NC	NC	NC	↑	↑

Fig. 6 Relationships between energy-transduction and qE sensitivity. As determined by its sensitive components, PsbS and VDE, qE (and thus NPQ) will be a function of lumenal pH. As pH drops from 6.5 to 5.8, qE will continuously increase to saturation. If the steady-state pH of the stroma is constant, then qE will be a function of ΔpH. Therefore, factors affecting the extent to which ΔpH forms will influence qE induction. Depicted are simplified schematics of chloroplastic energy transduction with proton and electron fluxes indicated in blue and red, respectively. The table indicates relative changes in ATP output, NADPH output, pmf, and ΔpH (NC indicates no change). The pmf (and by extension ΔpH) will depend, in part, on the steady-state rate of proton accumulation. Supplementing the rate of proton accumulation through CEF1 (A) or WWC (B) will increase pmf, the rate of proton efflux and, consequentially, the rate of ATP synthesis. However, since electrons on the reducing side of PSI return to the PQ/PQH_2 pool via CEF1 or to water via WWC, NADPH output does not change. Since at steady-state, the rate of efflux will equal the rate of accumulation, pmf will also depend on how conductive the membranes are to proton flux. Thus, decreasing conductivity (C) will require an increase in pmf to balance proton accumulation with efflux.
Since the steady-state rate of proton flux does not change in proportion to electron flux to NADPH, the relative outputs of ATP and NADPH remain constant. Finally, if, under most conditions the ΔpH partition is approximately 50% of pmf, collapsing the electric field component through counterion movements (D) would require an increase in ΔpH to sustain steady-state proton flux. In all cases, the sensitivity of qE to LEF (qE/LEF) increases (Cruz et al. 2005).

PSII lacking chloroplasts of the bundle sheath cells of C4 plants or when the PSI complex is functionally separated from the PSII complex, as in cells with a high PSI/PSII ratio (Asada 1999).

Therefore, in C3 plants, the cyclic electron flow is unlikely to induce the proton gradient to down-regulate PSII, at least just after exposure to

environmental stress. Since the water-water cycle itself does not consume ATP, the proton gradient is effectively generated under any environmental conditions. Thus, the water-water cycle can respond even to a sudden change of environmental factors such as sunflecks. The linear electron flow for the photorespiratory pathway consumes ATP at a higher ratio of ATP/NADPH than does that for the Calvin cycle, and would not contribute to generation of the proton gradient. Furthermore, the water-water cycle itself can dissipate excess of photons using O_2 as electron acceptor without releasing O_2^- and H_2O_2 even when the physiological electron acceptors are not available. The water-water cycle first triggers the down-regulation of PSII and then dissipates excess of excitation energy by reducing O_2 to water. Further, the water-water cycle would supply additional ATP required for the photorespiration, which not only dissipates
excess of energy through the electron flow but also supplies the physiological electron acceptor of CO_2 to chloroplasts (Asada 1999).

Directly or indirectly, the WWC and photorespiration cause increased production of H_2O_2, which is removed by an extensive scavenging/antioxidant network (Apel & Hirt 2004;Arora et al. 2002;Asada 2006;Mittler 2002;Niyogi 1999). The capacity of these reactions to contribute to the dissipation of excess excitation energy (EEE) must be dependent upon the effectiveness of the AOS scavenging/ antioxidant network; otherwise, AOS production would result in oxidative stress leading to cell death (Asada 1999; Mittler et al., 2004).

Moreover H_2O_2 arising directly from the Mehler reaction or indirectly from photorespiration could initiate signaling in response to high light stress, (Chaves, Maroco, & Pereira 2003;Gechev et al. 2006;Gechev & Hille 2005;Mullineaux, Karpinski, & Baker 2006) regardless of its significance in the dissipation of EEE.

2. Aims

The first aim of these studies was the comprehension of the expression mechanism of violaxanthin de-epoxidase gene and its relation with other physiological parameters during photo-oxidative condition, caused by light stresses combined or not with drought.

The second objective was to get a deeper insight of the role of water-water cycle as trigger for cellular adaptation during light stress.

For these purposes, four different experiments were established: two of them consisted of summer field experiments (long-term stress) and two of short-term stress imposition in laboratory.

3. Material and Methods

3.1 Long-term stress

The study site of field experiments is located at an elevation of 27 meters in north Italy near Bologna (44°31’55,02”N 11°24’45,16”E; Fig.7).

Fig. 7 Sat view of the experimental farm of Cadriano where the long-term water stress was conducted

3.1.1 First experiment: drought stress under full light (2004)

Ten plants of strawberry tree (*Arbutus unedo*) were grown in pots of 15 L capacity containing a mixture of soil:sand (1:1 vol.) and kept under a clear plastic roof to avoid rainfall. Five plants were watered with 3 litres per day while for the other water supply was interrupted from 18 May to 1 of June 2004. Plant water status, chlorophyll fluorescence and VDE expression have been measured in fully developed leaves. For the last two measurements, leaves were collected, frozen in liquid nitrogen and stored at -80°C until analysis.

Leaf water potential was measured from a single leaf per plant; chlorophyll fluorescence parameters were calculated from the same leaf of each plant during all the experiment; and one leaf from each plant, with position and orientation similar to the leaf used for fluorescence measures, was sampled for gene expression analysis.

3.1.2 Second experiment: drought stress under two levels of light (2005)

For the second field experiment, forty plants of strawberry tree were grown as above.

Before the beginning of the experiment (4 May 2005), all plants had been placed under an open tunnel covered by a clear polyvinyl chloride sheet and normally watered; a net (50% density) shaded half of them. During the experiment (from 16 to 30 May), twenty plants (ten shaded and ten not-shaded) were drought-stressed by withholding water.

The result was a sampling group made from four different series of ten plants: watered in light, watered in dark, stressed in light and stressed in dark.

Plant water status, chlorophyll fluorescence, xanthophyll content and VDE expression were measured. Leaf water potential values were the mean of three leaves taken from three plants per treatment; xanthophyll content and gene expression were measured from two different leaves of the same plant,

collected from five plants per treatment; finally, fluorescence measures were carried out on the same leaf of each plant during all the experiment.

3.1.3 VDE gene expression analysis

3.1.3.1 Primer design

In order to analyse the expression of the violaxanthin de-epoxidase gene in *Arbutus unedo*, it was indispensable design a pair of PCR primers, because no previous work concerning the DNA sequence of this gene in strawberry tree was done.

Tab. 1 VDE sequences alignment with ClustalW (Thompson, Higgins, & Gibson 1994). Primers were built on the green zones. Gene accession numbers were as follow: *Spinacia olaracea* (AJ250433), *Oryza sativa* (AF468689), *Camellia sinensis* (AF462269), *Citrus sinensis* (AF444297), *Triticum aestivum* (AF265294).

```
CAMELLIA SINENSIS GGAAGAAATGTGTGCCCCAGAAATCTGATGTTGGCGAATTTCCTGTCCCTCATCCTAATG 661
CITRUS SINENSIS   GAAAGAAGTGTGTACCACTGAAATCTGATTTAGGGGAATTTCCTGTCCCTGATCCTGCCA 71
SPINACIA OLERACEA GAAAGAAATGCGTGCCTCAGAAGTCTGATGTTGGAGAATTTCCTGTTCCCGATCCTAGTG 637
TRITICUM AESTIVUM GCAAAAAATGTGTCCCCAAAAAGTCTGATGTTGGGGAGTTCCCTGTCCCCGATCCATCTG 648
ORYZA SATIVA      GCAAGAAATGCGTCCCACAAAAGTCCGACGTTGGCGAGTTCCCAGTCCCTGATCCATCCG 107
                  * ** ** ** ** **    ** ** **  * ** ** ** ** ** ** **  ****

CAMELLIA SINENSIS TTTTAGTTAGAAACTTTAACATGAAAGATTTCAGTGGGAAGTGGTTCATAACTAGTGGTT 721
CITRUS SINENSIS   TTCTAGTTAAAAGTCTTAACCTCAAAGACTTCAATGGGAAGTGGTACATTTCTAGTGGTT 131
SPINACIA OLERACEA TGCTCGTTAAGAGTTTCAACATGGCAGATTTCAACGGGAAGTGGTTTATAAGTAGTGGTC 697
TRITICUM AESTIVUM CCCTGGTCAAGAACTTCAACATGGCAGATTTTAGAGGCAAGTGGTACATTTCAAGTGGCC 708
ORYZA SATIVA      CCCTTGTCAAGAACTTCAACATGGCTGATTTCAACGGCAAGTGGTATATTTCAAGTGGCC 113
                     * ** *  *   * *** *    ** ** *  ** *******  **    *****

CAMELLIA SINENSIS TAAACCCGACTTTTGATGCTTTTGATTGCCAACTGCATGAGTTCCATATGGAATCCAACA 781
CITRUS SINENSIS   TAAATCCTCCCTTCGATACTTTTGATTGCCTATTGCATGAATTCCATACAGAATCCAACA 191
SPINACIA OLERACEA TAAACCCTACATTCGACGCTTTTGATTGCCAGTTACATGAGTTCCATTTGGAAGATGGAA 757
TRITICUM AESTIVUM TAAATCCTACTTTTGACACGTTCGATTGCCAGCTTCACGAGTTTCGTCTCGAGGGAGACA 768
ORYZA SATIVA      TCAATCCCACTTTCGACACATTCGATTGCCAACTTCACGAGTTCCGTGTCGAGGGAGACA 119
                  * ** **  * ** **  * ** *******   * ** ** ** * *   **       *

CAMELLIA SINENSIS AACTTCTGGGGAACTCGACTTGGCGAATACGGACTCCAGACGGTGGCTTCTTTACGCGAT 841
CITRUS SINENSIS   AACTCATAGGAAATTTATCGTGGAGAATAAGAACTCCAGATGGTGGCTTTTTCACCCGAC 251
SPINACIA OLERACEA AACTTGTTGGAAACTTGTCTTGGCGAATAAAAACACCAGATGGTGGTTTTTTCACACGCA 817
TRITICUM AESTIVUM GGCTTGTTGCAAATTTGGCATGGAGAATTCCCACCCCGGACACCGGCTTCTTCACCAGGG 828
ORYZA SATIVA      AACTTATAGCGAACTTGACATGGAGAATTCGCACCCCCGACTCTGGCTTCTTCACCAGAA 125
                     ** * *  ** *   * *** ****    ** ** **    ** ** ** **  *

CAMELLIA SINENSIS CAGCTGTTCAGAGATTTGTGCAAGATCCTACTCAGCCTGCGATACTCTACAATCATGACA 901
CITRUS SINENSIS   CAGCTATGCAGAGATTTTTTCAAGATCCAATTCATCCTGGGATACTCTATAAACACGACA 311
SPINACIA OLERACEA CTGCTGTACAGAAATTTGCGCAAGACCCCTCTCAACCTGGAATGCTGTATAATCATGACA 877
TRITICUM AESTIVUM GGGCCGTGCAGCGGTTCGTACAGGATTCCTCACAACCAGCAATATTGTATAACCATGACA 888
ORYZA SATIVA      CAGCCATACAGCGGTTTGTGCAGGACCCAGCACAACCCGCGATCCTCTATAACCATGACA 131
                  **  * ***   **    ** **  *    ** ** *  **  * ** ** ** ****

CAMELLIA SINENSIS ATGAATATCTCCATTACCAAGATGACTGGTATATTT------------------------ 937
CITRUS SINENSIS   ATGAATACCTTCACTATAAAGATGACTGGTATATAT------------------------ 347
SPINACIA OLERACEA ATGCATATCTTCACTATCAAGATGATTGGTACATCC------------------------ 913
TRITICUM AESTIVUM ACGAGTACCTGCACTATCAGGATGACTGGTACATTC------------------------ 924
ORYZA SATIVA      ACGAGTTCCTGCACTATCAAGATGACTGGTATGTCCCTTAGATAGCACCTTCTGACGCTG 137
                  * *  *  ** ** **  * ***** ****  *  *

CAMELLIA SINENSIS ---------------------------------------------TGTCCTCCAAGATAG 952
CITRUS SINENSIS   ---------------------------------------------TGTCATCCAAGATAC 362
SPINACIA OLERACEA ---------------------------------------------TATCTTCTAAAATTG 928
TRITICUM AESTIVUM ---------------------------------------------TCTCATCGAAAATAG 939
ORYZA SATIVA      TACTTCAGATTTATTACTAAGATTTTCTGAAATGTAGGTACATTATCTCATCCAAAGTAG 143
                                                                 * ** ** **  *
```

```
CAMELLIA SINENSIS AGAATAAACCGGATGACTATGTATTTGTATATTATCGAGGCAGGAACGATGCATGGGACG 101
CITRUS SINENSIS   AGAACGAACCAGATGACTATGTCTTTGTGTACTATCGGGGCAGCAAT------------ 409
SPINACIA OLERACEA AAAATCAACCAGATGACTACGTATTTGTATATTACCGAGGCAGGAATGATGCGTGGGATG 988
TRITICUM AESTIVUM AGAACAAGGACGATGACTACATATTTGTATACTACCGTGGAAGAAATGATGCATGGGATG 999
ORYZA SATIVA      AGAACAAGGAAGATGACTACATTTTCGTGTACTACCGCGGCAGAAATGATGCGTGGGATG 149
                  * **  *   ********  * ** ** ** ** ** ** ** **
```

The conserved regions of this gene were located using known homolog sequences (Tab. 1), and a set of primer was chosen. Among these, the best options, scored by FastPCR software (ver 3.1.41 Institute of Biotechnology, Helsinki, Finland), were realized. The primer specificity was tested by sequencing the amplicon obtained. BLAST analysis showed a high grade of similarity between this sequence and other known VDE genes. The probability that such similarity has been determined only by chance was close to zero (E value = $7e^{-7}$) so this *Arbutus* sequence was used to design a second primer pair suitable for quantitative PCR (Tab. 2).

Tab. 2 Primers used for quantitative amplification of violaxanthin de-epoxidase gene of strawberry tree

5’- CCA TNG TAA GAG TAT CCC AGA GAT GC-3’
5’- ACT TTT AAT TGC CAA CGC CCT G-3’

3.1.3.2 RNA isolation and cDNA synthesis

Isolating high-quality RNA from some tissues, like strawberry tree leaves, is very difficult due to large quantities of polysaccharides and polyphenolic compounds that accumulate and co-purify with the RNA.

At the beginning, numerous different RNA extraction protocols were utilized on *A. unedo* leaves but the quality of the extract was too low, as consequence the samples of the first field experiment (one leaf per plant for each of the five sampling day) cannot be used for the quantitative study of VDE gene expression.

After numerous attempts, a suitable protocol has been developed and this made possible qPCR analysis for the second field experiment and for the short-term stresses.

This protocol was derived from a previous method (Meisel et al. 2005) applied on peach.

CTAB, high salt concentrations (NaCl) and polyvinylpyrrolidone (PVP40) has been used to get a pure RNA from *Arbutus* leaves. The high quality of total RNA obtained, allowed functional genomics analyses such as RT-PCR analysis.

Briefly, 0,5 g of leaf were ground in the presence of liquid nitrogen. The frozen powder was quickly transferred in 6 ml of preheated (65°C) extraction buffer[1] and well mixed by vortexing the tube. The sample has been incubated at 65°C for 15 min vortexing several times to avoid the separation of tissue and extraction buffer. An equal volume of chloroform-isoamyl alcohol (24:1 v:v) was added and vortexed vigorously. The supernatant obtained after centrifugation (15 min at 13000 g) was transferred to a new tube. The sample was re-extracted with an equal volume of chloroform-isoamyl alcohol (24:1 v:v) and centrifuged as previously described. The supernatant was carefully transferred to a new tube.

One third volumes of 8 M LiCl were added to the supernatant, well mixed by inverting the tube and incubated overnight at 0°C. RNA was pelleted by centrifuging the sample at 15500 g for at least 35 min at 4°C. The supernatant was carefully discarded and the pellet was resuspended with 500 µl SSTE[2]. The resuspended pellet was then transferred to a microfuge tube and extracted with an equal volume of chloroform:isoamyl-alcohol to reduce residual contaminants. The aqueous phase was recovered after centrifugation for 10 min at 15000g at 4ºC. Two volumes of ice-cold 100% ethanol were added to the sample and RNA was precipitated at -80ºC for 30 min. The sample was centrifuge at 17000g for 20 min at 4ºC and

[1] 2% (w/v) CTAB, 2% (w/v) PVP (mol wt 40,000), 100 mM Tris-HCl (pH 8.0), 25 mM EDTA, 2 M NaCl, 0.05% spermidine trihydrochloride, 2% ß-mercaptoethanol (added just before use)
[2] 1 M NaCl, 0.5% SDS, 10 mM Tris HCL (pH 8.0), 1 mM EDTA (pH 8.0)

supernatant was removed. The pellet obtained was dried at room temperature and dissolved in DEPC-treated water. All utilised solutions were treated with DEPC as described by Sambrook (Sambrook, Fritsch, & Maniatis 1989) and autoclaved. Tris-HCl (pH 8.0), prepared with DEPC-treated water, was added to the appropriate solutions post-autoclaving.
The quality and quantity of RNA were spectrophotometrically verified and the samples were stored at -80°C.
Total extracted RNA was treated with Turbo DNA-free (Ambion, Austin, USA) and residual DNA contamination was evaluated by PCR with the RNA solutions as template and the housekeeping gene primers. Samples that gave any amplification were purified a second time with the DNase. Thereafter, 3 µg of pure RNA were utilised by M-MLV Reverse Transcriptase (Invitrogen, Carlsbad, USA) for first strand cDNA synthesis following manufacturer's instruction.

3.1.3.3 Routine PCR

For routine PCR, Platinum Blue PCR SuperMix (Invitrogen, Carlsbad, USA) has been used. It provides reagents for the amplification of nucleic acid templates, and includes blue tracking dye for subsequent gel analysis. Specific binding of the anti-Taq antibody inhibits polymerase activity at room temperature. Activity is restored after a denaturation step in PCR cycling at 94°C, providing an automatic "hot start" in PCR and improving specificity and yield.

3.1.3.4 Real-Time Reverse Transcription Polymerase Chain Reaction (RT-PCR)

Many studies on the defence and stress mechanisms in plants have been based on gene expression (Chaves, Maroco, & Pereira 2003;Christmann et al. 2006;North et al. 2005;Reddy, Chaitanya, & Vivekanandan 2004;Rossel et al. 2006;Rossel, Wilson, & Pogson 2002) and transcriptome studies helped to provide a better understanding of plant stress responses. The

analysis of gene expression requires sensitive, precise, and reproducible measurement for specific mRNA sequences and the reverse transcription polymerase chain reaction (RT-PCR) is the most sensitive method for the detection of specific mRNA. In contrast with older techniques, such as Northern blot analysis and RNase protection assays, which require large amount of total RNA, RT-PCR assay is capable of quantifying mRNA levels from samples as small as individual cells. The introduction of fluorescence techniques to PCR, together with instrumentation able to amplify, detect and quantify low mRNA levels, has formed the basis of kinetic or real-time RT-PCR assays.

Quantification of mRNA transcription by real-time RT-PCR can be either absolute or relative. Unlike endpoint RT-PCR, real-time quantification is defined by C_t (threshold cycle number) at a fixed threshold where PCR amplification is still in the exponential phase and the reaction components are not limiting gene amplification. Two relative quantification method, the standard curve method and comparative C_t method, have been developed. In the standard curve method, the input amount for unknown samples is calculated from the standard curve of a specific gene, and normalized to the input amount of a reference gene (see function 1), which is also calculated from its standard curve.

With the comparative Ct method, the amount of an amplicon generated from the target gene is expressed as a ratio between the treated sample and the control and it is normalized to an endogenous reference, resulting in the fold difference between sample and control.

$$\text{ratio} = \frac{(E_{target})^{\Delta Ct\ target\ (control\text{-}treated)}}{(E_{ref})^{\Delta Ct\ ref\ (control\text{-}treated)}}$$ Function 1

E_{target}= efficiency of PCR amplification of the target gene

E_{ref}= efficiency of PCR amplification of the reference gene

ΔCt= difference between control Ct and treated Ct

When there are several treatments to compare, it is possible to calculate a mean normalized expression (MNE) of the target gene normalized to the reference gene through the formula

$$MNE = \frac{(E_{reference})^{Ct_{reference}}}{(E_{target})^{Ct_{target}}}$$ Function 2

To avoid bias, RT-PCR must be referenced to an internal control gene. Ideally, the condition of the experiment should not influence the expression of this internal control gene. Currently, at least nine housekeeping gene are well described for the normalisation of expression signal (Nicot et al. 2005). The most common are actin, glyceraldehydes-3-phosphate dehydrogenase, ribosomal genes, cyclophilin, and elongation factor 1-α (ef1α).

The majority of studies in the literature uses a unique internal control, which often is actin. However, a reference gene with stable expression in one organism may not be suitable for normalization of gene expression in another organism under a given set of condition and needs to be validated before its use. Nevertheless, in recent studies 18S rRNA was found as most reliable reference gene for normalization in many plants (Jain et al. 2006;Nicot et al. 2005) but a correct cDNA dilution should be done to bring its measurement in the dynamic range of RT-PCR despite to its extremely high level of expression.

The SYBR GreenER qPCR SuperMix for ABI PRISM instrument (Invitrogen, Carlsbad, USA) was used: the reaction mixture consisted in a reaction volume of 25 µl, containing 1µl of cDNA obtained from *Arbutus unedo*.

The qPCR measures were obtained through an ABI Prism 7000 Sequence Detection System (Applied Biosistem, Foster City, USA) in 96-well plates,

thermal cycling parameters were set accordingly to manufacturer's instruction.

Ribosomal 18S gene was used as housekeeping gene in all the qPCR measure made in *Arbutus unedo*.

3.1.4 Xanthophyll analysis

This analysis was performed only for the second long term experiment. On selected days, leaf samples were collected for the determination of xanthophyll content and de-epoxidation state.

Leaves were collected from each of five plants per treatment at predawn and at midday. Leaves were frozen in liquid nitrogen and stored in the dark at -80°C until extraction.

Leaves were then ground in a mortar in liquid nitrogen, under dim light, and the collected powder was extracted with 1.5mL cold HPLC grade 100% acetone. In order to avoid traces of acid in the acetone used for the extraction, 0.5 g/L of calcium carbonate were added (Garcia-Plazaola & Becerril 1999).

Extracts were centrifuged at 5000 x g at 0°C for 4 min and the supernatants were stored in ice. The pellets were re-suspended with small amounts of acetone (e.g. 0.5 mL) until the supernatants remained colourless. Water was added to the combined supernatants to give a final concentration of acetone 80% (v/v). The pigments solutions were finally filtered trough a 0.45 µm syringe-filter (Chemtek Analitica, Bologna, Italy) and stored in the dark at -20°C until injection into HPLC. To avoid any possible sample degradation or concentration by solvent evaporation, injection was made within two days from extraction.

Pigments composition was analysed with reversed-phase HPLC according to Niinemets et al. (1998) using a Hypersil ODS column (particles size 5 µm, 250 mm x 4.6 mm; Alltech Italia, Sedriano, Milan, Italy), which was termostated at 15°C, in combination with a guard column (5 µm, 7.5 mm x

4.6 mm). The HPLC system was equipped with two pumps LC-10AD, a mixer FCV-10AL model, a oven CTO-10AS and a degasser gastorr 154 (Shimadzu Italia, Milan, Italy), and an UV6000 LP photodiode array detector by Finnigan SpectraSYSTEM (Milan, Italy).

The pigments were eluated at a flow-rate of 1.5mL min-1. Two solvents with different polarities were used for separation: solvent A: Tris(hydroxymethyl)aminomethane Buffer pH 8.0 10mM, and solvent B: acetone HPLC grade 100%. The mixture of 75% solvent B and 25% solvent A was run isocratically for the first 7.5min, followed by a linear gradient to 100% B for the next 9.5min. Then, solvent B runs isocratically for 3 min. This was followed by a change in the eluent composition to 25% A and 75% B with a linear gradient for 2 min and then the column was equilibrated for 8 min before the next sample injection. The injection volume was 20 µL. For overnight storage the column was flushed with methanol: water (50/50, v/v).

Peaks were detected and integrated at 445 nm for carotenoid and chlorophyll b content, and at 410 nm for chlorophyll a and pheophytin a. Their concentrations were calculated from the corresponding peak area units to µmol per injection (Munne-Bosch & Alegre 2000). We calculated the conversion state of the xanthophyll cycle as the ratio (Z + 0.5A)/(V+A+Z), following (Muller et al. 2006).

The calibration was performed using commercially available pigments standards (DHI Water & Environment, Denmark). The calibration factor for violaxanthin (V) was also used for antheraxanthin (A). Standards of lutein were injected periodically in order to correct the conversation factors, assuming that the extent of changes would be the same for all coefficients, as described by (de Las Rivas, Abadia, & Abadia 1989).

3.1.5 Chlorophyll fluorescence analysis

This analysis was performed in both long-term experiments. Calculation of useful fluorescence parameters irrespective of the method used to perform

the analysis requires the knowledge of the state of the photosynthetic system. With dark-adapted material, the F_0 level of fluorescence is recorded at very low PPFD (generally less than 1μmol m^{-2} s^{-1}), which leaves virtually all PSII centres in 'open' state (capable of photochemistry). The Fm level of fluorescence is recorded during a short pulse at very high PPFD (typically less than 1 s at several thousand μmol m^{-2} s^{-1}), which transiently drives a very high proportion of PSII centres into the 'closed' state (making the capacity for photochemistry close to zero). With light adapted material, the equivalent terms are F'_0 and F'_m. At any point between F'_0 and F'_m (where a variable proportion of PSII centres are in the 'open' state), the fluorescence signal is termed F'. The difference between F_m and F_0 is termed F_v and the difference between F'_m and F'_0 is termed F'_v. While F_v and F'_v have been widely used for a number of years the specific term F'_q has recently been introduced to denote difference between F'_m and F' measured immediately before application of the saturating pulse used to measure F'_m (Fig. 8).

F'_q/F'_m is theoretically proportional to the operating quantum efficiency of PSII photochemistry (hereafter referred to as PSII operating efficiency).

During each field experiment, chlorophyll fluorescence has been measured with a portable fluorometer PAM 2000 (Waltz, Effeltrich, Germany). A single strawberry tree leaf per plant was used and the PSII maximum efficiency (Fv/Fm) was assayed before sunrise (approx. from 4:30 to 5:00 am). A second fluorescence measure was taken on the same leaf at noon, when F'v/F'm was calculated after few second of complete leaf darkening obtained with a black fabric pocket.

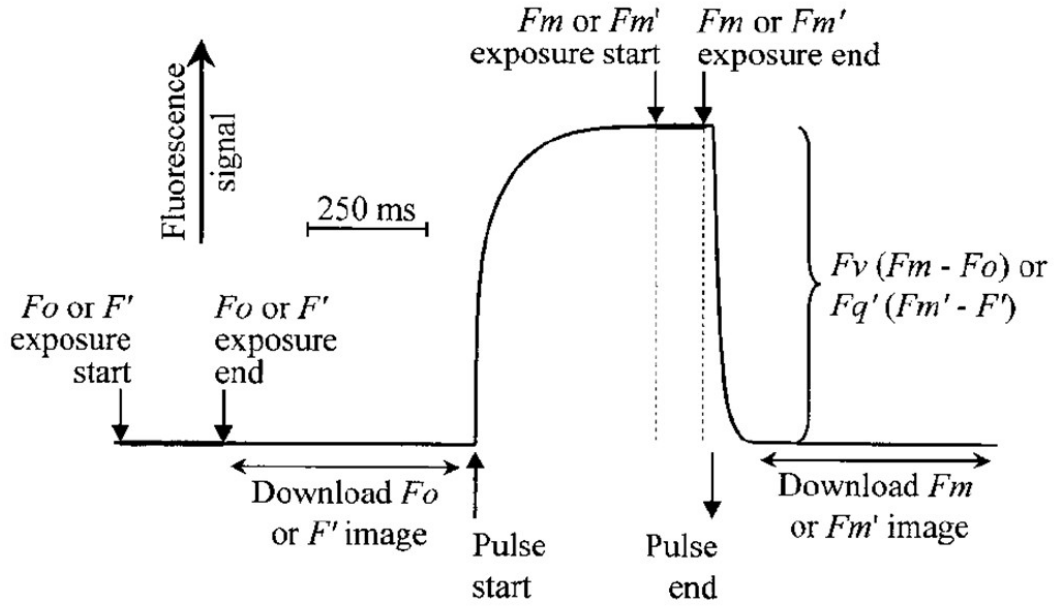

Fig. 8 Fluorescence trace illustrating the terminology used and the sequence of events leading to the acquisition of the raw fluorescence images that are required for the construction of parameterized images.

3.1.6 Leaves water potential

Leaf water potential (LWP) was measured from at least three leaves per treatment with a pressure chamber (model 3000, Soil Moisture Equipment Co., Santa Barbara CA USA) before the dawn on a basal and fully expanded leaf.

3.2 Short-term stress

Light stress was imposed on both *Arbutus unedo* and *Arabidopsis thaliana*. Strawberry tree plants were of the same age and size of those used for the long term stress.

Arabidopsis plants (ecotype Columbia [Col-0] and *cds1-2*) were grown, after seed vernalization, to mature rosette stage (5 weeks after germination)

under controlled environmental condition (PPFD 150μmol $m^{-1}s^{-1}$) with a 8-h photoperiod at 23°C and a relative humidity of 60% (Fig. 9).

Fig. 9 Panel A: 5-week old Col-0 plants Panel B: *cds1-2* plant of the same age

The *cds1-2* mutant has a t-DNA insert in the promoter of Cu/Zn chloroplastic Superoxyde dimutase (chl-Cu/ZnSOD). This insertion results in the suppression of chl-Cu/ZnSOD expression at the RNA and activity levels (Rizhsky, Liang, & Mittler 2003c) and in a less efficient water-water cycle.

An artificial light source made up of several halogen lamps (1300 Watts total) has been mounted on the top of a framework supporting an heat filter consisting in an open, water filled chamber (Fig. 10).

The experiments have been performed indoor with a constant temperature of 25°C, the radiation measured in the working zone (where the leaves were collected) was between 1000 and 1500 μmol $m^{-2}s^{-1}$ but no significant variation of the leaf temperature was detected during the light stress. This apparatus was used with both *Arbutus* and *Arabidopsis* modifying the length of excess light period: 60 minutes for *Arabidopsis* and 6 hours for *Arbutus*. The different lengths of the light stress were chosen in order to obtain a severe but not irreversible response from the plants.

Chlorophyll fluorescence, xanthophyll content and VDE expression were measured at four different time points (0 min, 10 min, 30 min, 90 min and 360 min) in strawberry tree plants. The same physiological parameter, and the expression levels of a pool of light-activated genes, were measured on

Arabidopsis plants before and immediately after the stress imposition (60 min).

Fig. 10 Light-stress apparatus. Halogen lamps were fastened on the top of the structure immediately over the heat filter. The rubber tubes that assured cold water circulation are visible on the right. An electric fan kept a constant air flow through the lamp avoiding bulb over-heating.

3.2.1 VDE gene expression analysis

3.2.1.1 Primer design

The primer pair for VDE gene amplification in *Arbutus* was previously described.

The sequence of *Arabidopsis* VDE gene was well known and the chosen primer pair was the best option found by the Fast PCR software (ver. 4.0.27) which gave an amplicon of around 200 bp (Tab. 3).

Tab. 3 Primers used for quantitative amplification of violaxanthin de-epoxidase gene of *Arabidopsis*

5’- TTC GAC TGC CAG CTG CAT GAG-3’
5’- TCT CCA CGA GCG CAG GTT CAG-3’

The primers used for the light responsive genes were previously described (Bechtold et al, submitted) and are reported in table 4.

Tab. 4 Primers used for quantitative amplification of light responsive *Arabidopsis* genes

		Primers	
		Forward	Reverse
AT4G13770	cytochrome P450 monooxygenase	5'AGGTTTCTTGAGAAGGAAGTTG3'	5'GAAACCAAACATTGAAACAGAA3'
AT1G52400	beta-glucosidase homolog (BG1)	5'AAAGTGAACGTTACGGGATACT3'	5'CTAACATAGGAAGGACCGGTAG3'
AT1G76790	O-methyltransferase	5'CAAGAATTGTTGGAAAGCATTA3'	5'TTATTACCATGAGACGGTTCAC3'
AT5G24770	vsp2	5'AGGAAGAGTCTCGTGAAGAAAG3'	5'CACAACGGCTACAAAGATAAAC3'
AT1G21250	wak1	5'GAACGAGGATAATCTGAAGGAG3'	5'TATTGATGAAGCAACAAAGAGG3'
AT1G21270	wak2	5'CAGAGTTAGAGGCCTTGAGAGT3'	5'TTATTGATGAAGCAACAAGGAA3'
AT1G35710	LRR XI	5'GTGTTTACAAGCAAATCCAGAA3'	5'AACCAAACACATTACAAGACCA3'
AT1G58270	At1g58270	5'TGCAAATGATAGAAACCTGTCG3'	5'CCAATGGAGTTGGAAATGCT3'
AT3G09840	CDC48	5'AACGTCTGAGCAAAGGCTTG3'	5'TTGCAAGTACGCCATCAGAG3'
AT3G45970	Espansine	5'CGCAAGGATCACAACCTTCT3'	5'TACATGACAAGAAGCCACGG3'
AT4G21580	Quinone-NADPH oxidoreductase	5'CCAAGAAGCCCTGAAAACAA3'	5'GCTCTGACATTCTCCCTTGC3'
AT5G61510	quinone oxidoreductase	5'AAGAGCGACTTTGGAGCAAG3'	5'GGATTTTGTTTCCCGAGTCA3'
AT4G10040	cytochrome c	5'CCATTTTTGTTCCAGGGATG3'	5'GTCACACCGTCGAGAAAGGT3'
AT2G26140	ATP-dependent zinc protease	5'GCAAAAACAATCCTCACGGT3'	5'GATGCTGACCTAGGGGTTGA3'
AT5G22060	DNAJ	5'ATGAAATGTGGTGGCTGTCA3'	5'TGGAATCCCTTCTCCACATT3'
AT5G03030	DnaJ protein-like	5'CAAGCTTTCAAGGCAAGACC3'	5'ATAGTGACTGCCTCCAGCGT3'
AT5G56000	heat shock protein 81.4	5'CCAAGGAAGGTCTGAAGCTG3'	5'CTCTCCATGTTTGCAGTCCA3'
AT4G24280	HSP	5'GCATCGATCACATCATCACC3'	5'GGAAGTGGATCAACCCAAGA3'
AT4G26160	Thioredoxine	5'ATGCAGCTGGTTTGGCTAAT3'	5'CCGATGTGCAAGAGTTTGAA3'
AT1G07360	RNA binding protein	5'GTTGAGAGGATCCCGAAGGT3'	5'ATATGCCATCGCCTTACCAG3'
AT4G03430	splicing factor	5'TCGGCTCACAAGCTACACAC3'	5'TCACCATAGCTGTTGCCAAG3'
AJ242484	FKBP like protein	5'CAACACCATTCAGAAACCCC3'	5'TTAAGGGATGGGATGTTGGA3'
AT5G58590	Ran binding protein 1 homolog (RanBP1)	5'TCCTTTGCAGGCTCTTTCTC3'	5'GCATTCGATTTGCTTCCATT3'
AT4G35090	CAT	5'CCAGCTTCTGTCCCAAAGAC3'	5'GGAAAACGTGAGAGGTGCAT3'
AT1G78380	glutathione transferase	5'GTTTGGAATGAGGACGAGGA3'	5'TTTGCTAGGCCAAACTTCGT3'
AT5G45870	PR protein	5'ACACCATAAAGACTGAACATTTG3'	5'AATAACATCAATCTCAATCATTCG3'
AT1G76880	DNA binding protein	5'TTCTGTTCCCTTGATGGTCC3'	5'CAAGCTCGAACTCACCTCCT3'
AT4G28140	DNA binding protein	5'GCCATACCTTCCTCTCTCCC3'	5'GCCAAGCCTTCAAATTACGA3'

AT1G14200	zinc finger protein family	5'CCCTAACCACTCCTCCACAC3'	5'GATTTCTTTAGCGACGGTGG3'
AAF26770	vacuolor sorting protein	5'CTCCGGCTGTTGAAAGTCTC3'	5'TCAAGCTCGGATGTTTTTGA3'
AT1G32230	WWE	5'AAAGGAGAACCACAAAGGCA3'	5'AAACTGCGGGTGATTGTAGG3'
AT1G52870	peroxisomal membrane protein	5'CTAAAACCTCACCGTTCCCA3'	5'CACTCGTCGCAGCACTAAAA3'
AT2G01190	PB1 containing protein	5'TCACAATGGCTGTGAACTCC3'	5'GTCTGGTTCAGCTGGGAATC3'
AT3G03270	USP	5'TTCACGTCCAACCACAAAAC3'	5'TGGATCACCCCAATACACCT3'
AT4G23885	expressed protein	5'AATGATCAGATGCAGCCTCC3'	5'CTCGCATCAAATTCCCTCAG3'
AT5G64400	At5g09570	5'CCAATCACGGAACCAGAGTT3'	5'TTCAGCATGAGGCTGTTGAG3'
AT5G10695	At5g10695	5'AATGATCTCGTATGAGGTGGG3'	5'GAGAGGGTGATCGGAAGGTA3'
U27698	Calreticulin	5'AAGATGGTGAGTGGACTGCC3'	5'ATCCTGATTTCACCTGCCAC3'
AT3G02040	SRG3 protein	5'TGAAGGGAGTATTCCGCAAC3'	5'AGCATCTCTGTTGGATGGCT3'
AT4G17460	leucine zipper protein-like	5'CATGATGATGGGCAAAGAAG3'	5'CCTCGCAGTTAACCGTTGAT3'
AT5G58070	Lipoprotein	5'ACCTTCCTCCACTGCCTTCT3'	5'CAAGCTCAAAGTCCCGTTTC3'
AT1G35140	phosphate-induced (phi-1) protein	5'CGATTTCGTTGCTTCCTCTC3'	5'GCTAGTTTGCCACTTTTCGC3'
AT4G04020	Fibrillin	5'TTCAATGGTGGTTGGTTTGA3'	5'CGAAGTCCCTAAACGTGTCC3'
AT3G22840	ELIP1	5'CCGGTAGCTTCCCTAACCTC3'	5'CCGCTAAACGCTAGCAAGTC3'
AT5G25450	ubiquinol-cytochrome-c reductase	5'GAGAGGTAAAGCTCCCAAAGC3'	5'TAATTCCACAGGCAGTGCAG3'
AT2G32920	disulfide isomerase	5'TCACGATCTCTGGTGTTCCA3'	5'GTGGCGGCTGTAACTCAAAT3'
AT1G53540	heat shock protein 17.6	5'CTGGATGTTTTCGATCCGTT3'	5'ATGTTGCCATCCTCAACCTC3'
AT3G23990	heat shock protein	5'TCCTGACTCGCTTTCGTCTT3'	5'ATTGTTGGCAAGCTCTTGGA3'
AT4G24280	heat shock protein 70	5'TGGCTCTACAAGGATTCCCA3'	5'TTCCAAACCCAAGGACAGAG3'
AT2G29500	HSP	5'CATCGCAGCCTTAACCTGAT3'	5'CTTGCCTGGATTGAAGAAGG3'
AT3G25230	FKBP62	5'GAGCAACGCCTTTCAAATTC3'	5'GCCTTCACACTGTCCCATTT3'
AT2G47730	glutathione transferase	5'GCGAGAGTCAAAGAGCACCT3'	5'TCTTTAAAGGCATGTTCGGC3'
AT3G58680	ER24	5'AACCTTCTCCATCTTCGCAA3'	5'AAGAAGAAACAGACTGCGGC3'
AT2G46830	CCA1	5'TCAAAAACGGGTGTGAATGA3'	5'TGCTTGCGTTTGATGTCTCT3'
AT1G30070	SGS domain-containing protein	5'TGCGCCAACATTTGACTAAA3'	5'GCTAAAGCCTGGACAGATGC3'

3.2.1.2 RNA isolation and cDNA synthesis

TRIzol (Invitrogen, Carlsbad, USA) was used according to manufacturer's instructions to isolate RNA from *Arabidopsis* leaves starting from 500 mg of frozen material.

RNA purification from *Arbutus* and cDNA synthesis were conducted as previously described for long-term experiments.

3.2.1.3 Real-Time Reverse Transcription Polymerase Chain Reaction (RT-PCR)

SYBR Green Jump Start Taq Ready Mix (Sigma, Saint Louis, USA) and SYBR GreenER qPCR SuperMix for ABI PRISM instrument (Invitrogen, Carlsbad, USA) were used with *Arabidopsis* and *Arbutus*, respectively.
Gene expression values of Arabidopsis were normalised with actin gene as internal control while ribosomal 18S gene was utilized for VDE expression in Arbutus.

3.2.2 Chlorophyll fluorescence analysis

Arabidopsis chlorophyll fluorescence has been measured with an instrument first described in (Oxborough & Baker 1997) and subsequently further developed (Baker et al. 2001;Fryer et al. 2002). This instrument, called Fluorimager, can measure and calculate fluorescence parameters for the whole rosette at once, and display it immediately through a false colour image.
Measures of PSII maximum efficiency and F'_q/F'_v were taken for each plant before and after the light stress respectively

3.2.3 ROS Imaging and quantification

Infiltration of leaves with nitroblue tetrazolium (NBT- Sigma, Saint Louis, USA) allowed the detection of superoxide. When the pale yellow NBT reacts with superoxide a dark blue insoluble formazan compound is produced. Superoxide is thought to be the major oxidant species responsible for reducing NBT to formazan (Fryer et al. 2002).
Fully expanded leaves were used thanks to the long petioles that made possible an easy handling of the two successive underwater cuts required to avoid air entering in the veins. These detached leaves were allowed transpirationally to imbibe aqueous solutions of NBT (5 mg/ml for *Arabidopsis*, 1.25 mg/ml for *Arbutus*) until completely infiltrated (approx. 90 minutes for *Arabidopsis*, overnight for *Arbutus*) at the growth light

environment. Solutions were replaced with water during the following stress period.

In order to obtain an image of superoxide distribution into leaf tissues, chlorophyll was removed from intact leaves by washing them with lacto-glicerol-ethanol (1:1:4 v:v) at 90 °C. The dark green *Arbutus* leaves required fresh washing solution after the first 15 minutes and some pigment retention was however visible at the end of the treatment. Decoloured leaves were placed on laboratory paper and slowly air-dried. Images were acquired through a high-resolution flatbed scanner.

The same colouring procedure was followed to obtain a quantitative measure of superoxide content but at the end of the stress, leaves were ground in liquid nitrogen. The samples were then washed twice with acetone (100% and 80% respectively) after a brief dark incubation (15 min) and centrifuged at 20000 g for 12 min. Pellets were dissolved in 700µl of DMSO and 50 µl of 0,1 M NaOH were added to solubilize the formazan. Samples were again centrifuged to pellet debris and the supernatants were used in combination with a Spectrophotometer ND-1000 (Nanodrop, Rockland, USA) for absorbance measure at a wavelength of 717 nm.

The Amplex Red Hydrogen Peroxide/Peroxidase Assay kit (Molecular probes, Eugene USA) has been used to quantify leaf hydrogen peroxide. In the presence of peroxidase, Amplex Red (10-acetyl-3,7-dihydroxyphenoxazine) reacts with H_2O_2 in a 1:1 stoichiometry to produce a bright pink oxidation product, resorufin. It has absorption and fluorescence emission maxima of 571 nm and 589 nm respectively.

Frozen leaf tissue (approx. 100 mg FW) has been ground in liquid nitrogen and 500µl of ice cold 0,1 M HCl were added. The samples have been centrifuged for 10 mins at 13.000 rpm at 4°C and then 5µl of the supernatant has been used for the assay, following the manufacturer's instruction. After a 45-minutes-long dark incubation, absorption was measured with a Spectrophotometer ND-1000 (Nanodrop, Rockland, USA)

3.2.4 Xanthophyll analysis

HPLC pigment analyses were conducted as previously described for the long-term stress.

Each *Arbutus* leaf was cut longitudinally in halves: one-half was processed for RNA extraction and the other half for HPLC analysis. Several *Arabidopsis* leaves, instead, were pulverized together in liquid nitrogen then half of the grinded material was used to purify RNA and the other half to quantify xanthophyll content.

4. Results

4.1 Long-term stress

In the **first field experiment** on *Arbutus*, the physiological state of the plants was monitored during the water stress. Leaf water potential (LWP) showed a small decrement during the first four days of water deprivation but, in the following days, a rapid decline of LWP exceeding the measuring capacity of the used equipment with estimated values of around -4 MPa was observed. Nevertheless, seven days after the end of water deprivation stress, both treated and control plants recovered and LWP was back to the values that precede the stress imposition (Fig. 11).

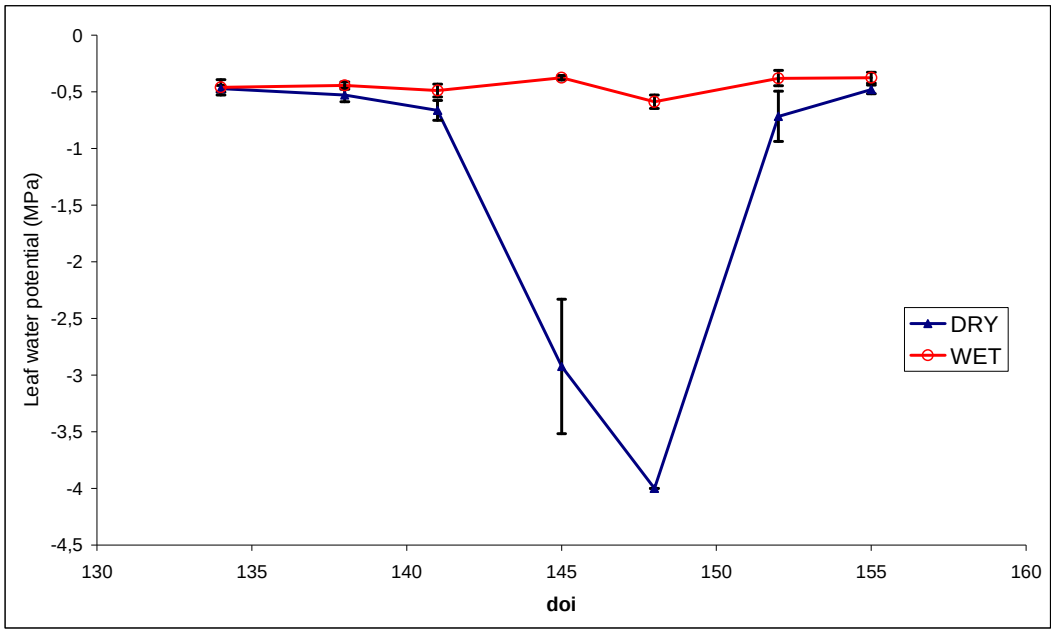

Fig. 11 Leaf water potential of watered and drought stressed plants. Water stress began on 18 May (doi 138) and last until 1 June (doi 152). Each point is the mean of 5 measures. Bars are SEs.

During the **second field experiment**, leaf water potential was again measured in the four treatments to monitor the physiological state of the plants. As previously observed, a two-step pattern was visible in the drought stressed plants: during the first few days of water deprivation LWP remained constant, then it showed a rapid decline which in the case of

Stressed-Light treatment exceeded the instrument measuring capabilities (Fig. 12).

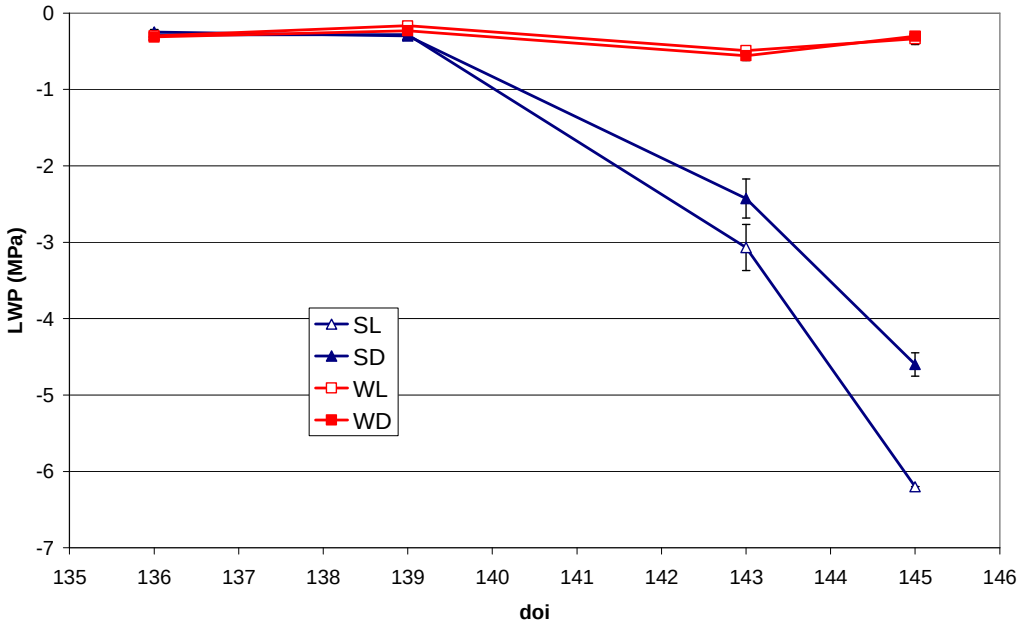

Fig. 72 Leaf water potential. SD: water stressed, dark environment; SL: water stressed, full light; WD: watered, dark environment; WL: watered, full light. Water stress began on the 16 May (doi 136).

4.1.1 VDE gene expression

It was possible to get only qualitative results of VDE gene expression during the first field experiment on *Arbutus* because of the poor quality of the RNA extract that did not permit to obtain reliable qPCR. Nevertheless, it was found that VDE gene is expressed only sporadically at midday in the watered plants throughout the experiment: in fact only 3 leaves, in a sampling group of 25, resulted positive for VDE mRNA. At the same time, the treated plants showed the highest number of plants expressing VDE gene at noon corresponding to the maximum drought stress (4/5 leaves positive for VDE mRNA on doi 148), while during all the stress period only half of the leaves expressed VDE gene at noon.

The development of a new and improved protocol for RNA extraction from *Arbutus unedo* made possible to get abundant RNA suitable for a quantitative analysis of gene expression by Real-Time PCR. Therefore,

during the second field experiment, VDE gene expression was studied through real-time PCR. The four different treatments showed a clear circadian pattern of expression with the highest value during the night, and remarkable differences between treatments (Fig. 13) during the experiment.

The ‘stressed-dark’ plants showed high VDE expression only during the night of the first part of the experiment.

The ‘watered-dark’ plants had a similar expression pattern but with a smaller expression during the first phases of stress period.

The ‘stressed-light’ plants displaied a very low level of VDE expression during all the experiment.

The ‘watered-light’ plants had a continuous and large increment in night expression level during all the experiment.

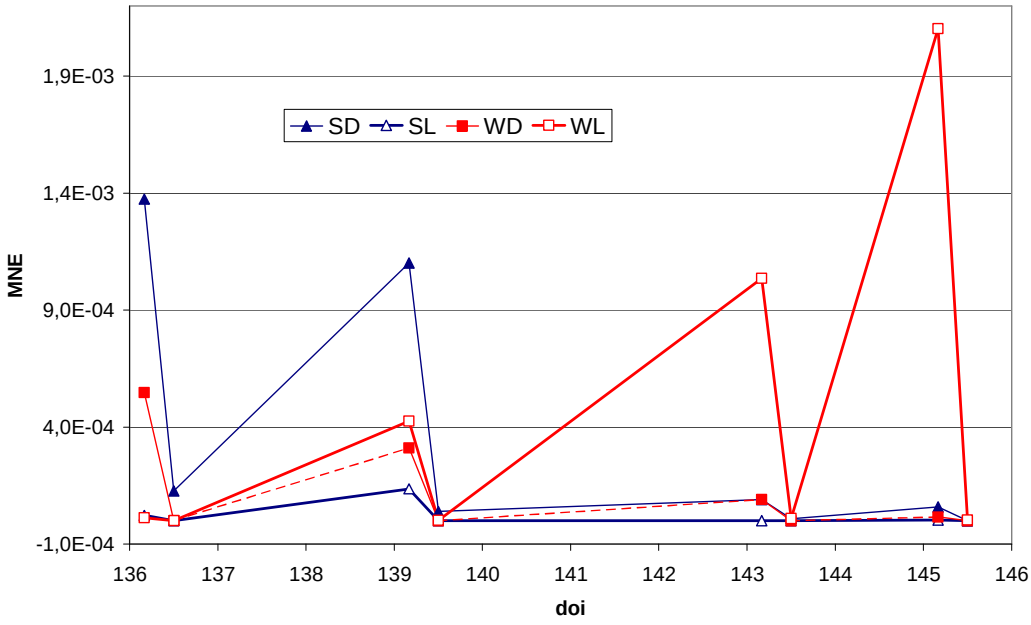

Fig. 13 Mean normalized expression (MNE) of VDE gene. Values are normalized with 18S gene expression. SD: water stressed, dark environment; SL: water stressed, full light; WD: watered, dark environment; WL: watered, full light. Water stress began on the 16 May (doi 136).

4.1.2 Xanthophyll analysis

Xanthophyll pool size and de-epoxidation state were measured in the four treatments of *Arbutus* plants during the second field experiment.

Light environment where the plants were kept before starting water deprivation affected leaf xanthophyll concentration. Indeed plants fully exposed to sunlight had a xanthophyll pool size that is twofold greater than that of shaded plants (Fig. 14). On the contrary, the small variations detected during the stress period suggest that drought stress have no effect on xanthophylls concentration (Fig. 14).

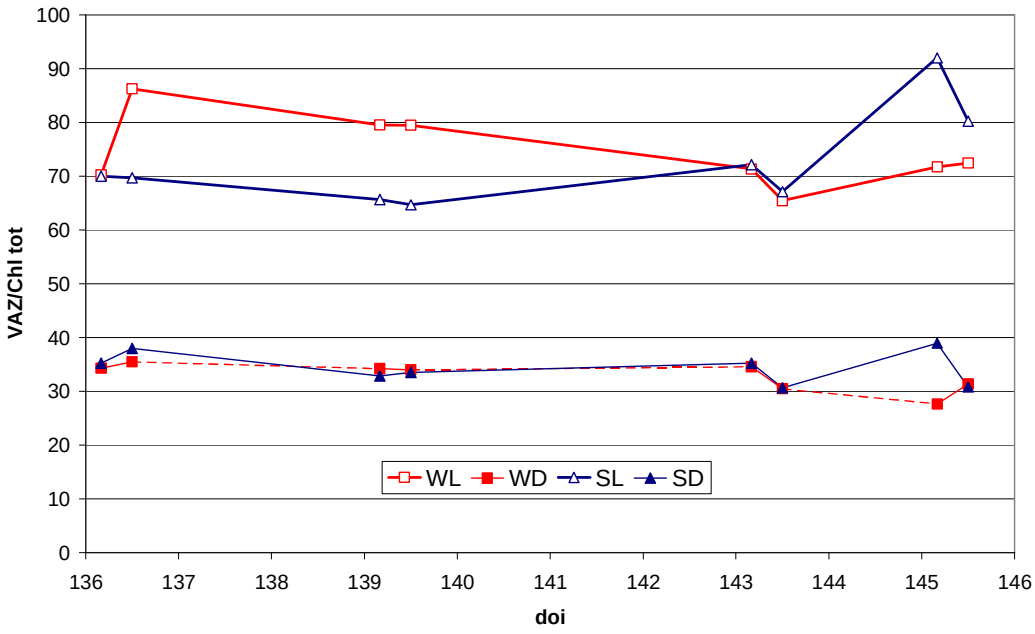

Fig. 14 Xanthophyll content normalized on chlorophylls. SD: water stressed, dark environment; SL: water stressed, full light; WD: watered, dark environment; WL: watered, full light. Water stress began on the 16 May (doi 136).

The de-epoxidation state (DEPS) of the xanthophylls, expressed as (V+0,5A)/(V+A+Z), had an unequivocal circadian pattern (Fig. 15). In the 'watered-light' plants, DEPS values were between 10% and 20% at dawn and reached 60% - 70% at midday with a slight increase in the midday values during the stress period. This increase was greater in the 'stressed-

light' than in watered-light plants: indeed after a first period with values similar to those of the 'watered-light' plants, there was a sudden increase in the midday DEPS values (86%). Predawn values in stressed-light plants showed a constant increment throughout the experiment. The same trend was observed in the 'stressed-dark' plants with some days of delay in the DEPS values increment at midday. Finally the 'watered-dark' plants did not show any noteworthy xanthophyll conversion and as consequence the DEPS values remain stable.

The presence of xanthophylls in their de-epoxidated form, even before dawn, and the structural damages to the photosystem protein complex could be the causes of the loss of the PSII efficiency that emerges from chlorophyll fluorescence data (Fig. 19) and that will be discussed later.

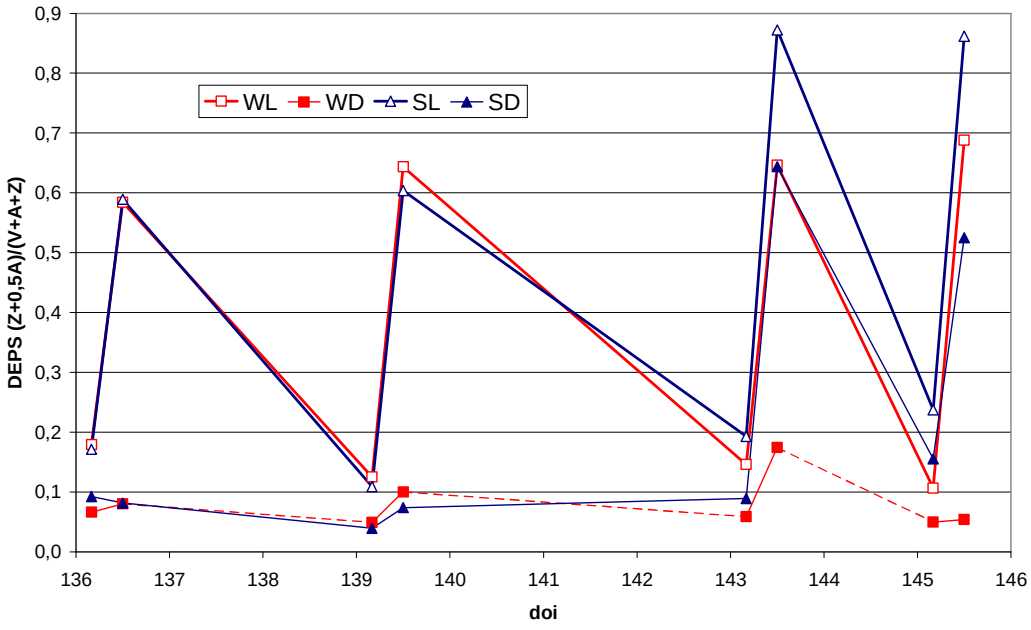

Fig. 15 De-epoxidation state of xanthophyll (DEPS) SD: water stressed, dark environment; SL: water stressed, full light; WD: watered, dark environment; WL: watered, full light. Water stress began on the 16 May (doi 136).

4.1.3 Chlorophyll fluorescence analysis

The first indications about how Arbutus plants behave during drought stress came from the 2004 field experiment. PSII maximum efficiency showed, in the drought-stressed plants, a clear fall during the stress period and a following fast rise. The recovery was complete after seven days when the stressed plants return to have PSII maximum efficiency values matching to the watered ones (Fig. 16).

Analyzing the single components of the maximum efficiency, it can be seen that the difference in Fv/Fm was largely due to the fluctuation of Fm (Fig. 17), while F0 variations were limited (data not shown).

This depression of PSII efficiency caused by water deficit is well known (Lu et al. 2003;Martinez-Ferri 2000;Muller et al. 2006;Muller, Li, & Niyogi 2001), but surprisingly it has been found a simultaneous decline in NPQ that is rapidly restored during the recovery (Fig. 18).

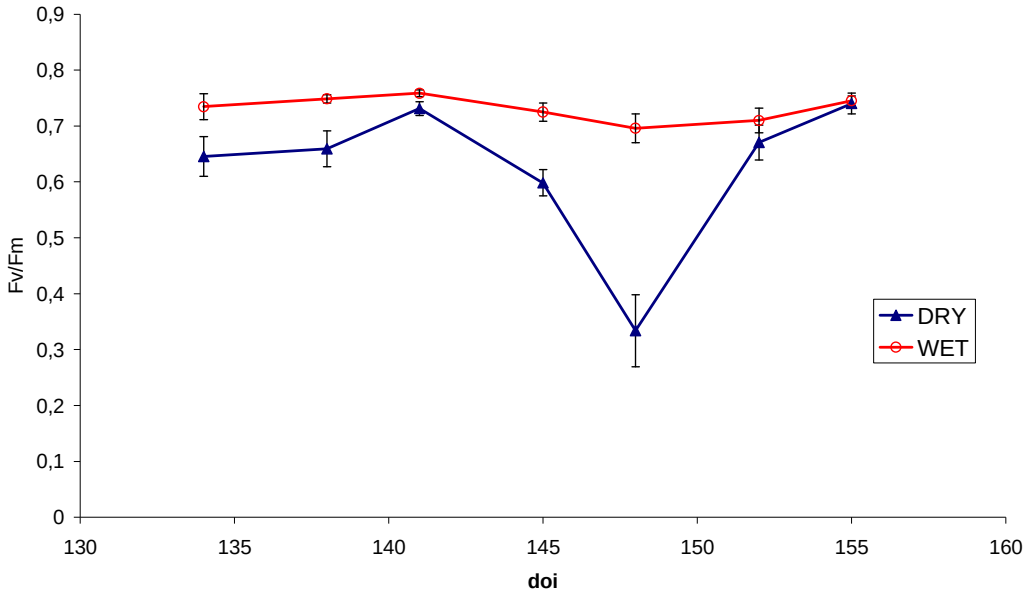

Fig. 16 Fv/Fm of watered and drought stressed plants. Water stress began on 18 May (doi 138) and last until 1 June (doi 152). Each point is the mean of 5 measures. Bars are SEs.

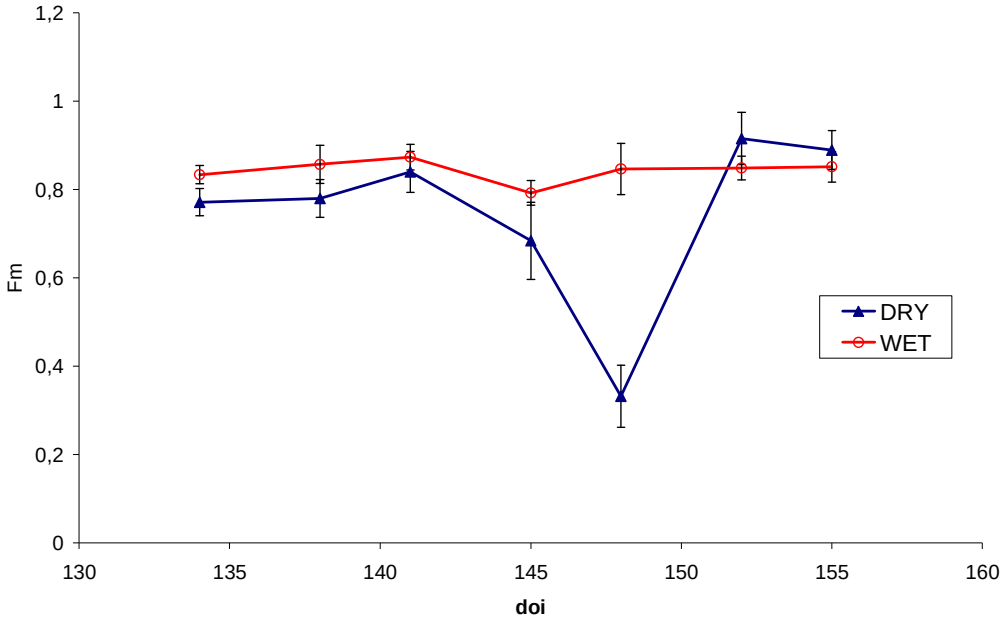

Fig. 17 Fm of watered and drought stressed plants. Water stress began on 18 May (doi 138) and last until 1 June (doi 152). Each point is the mean of 5 measures. Bars are SEs.

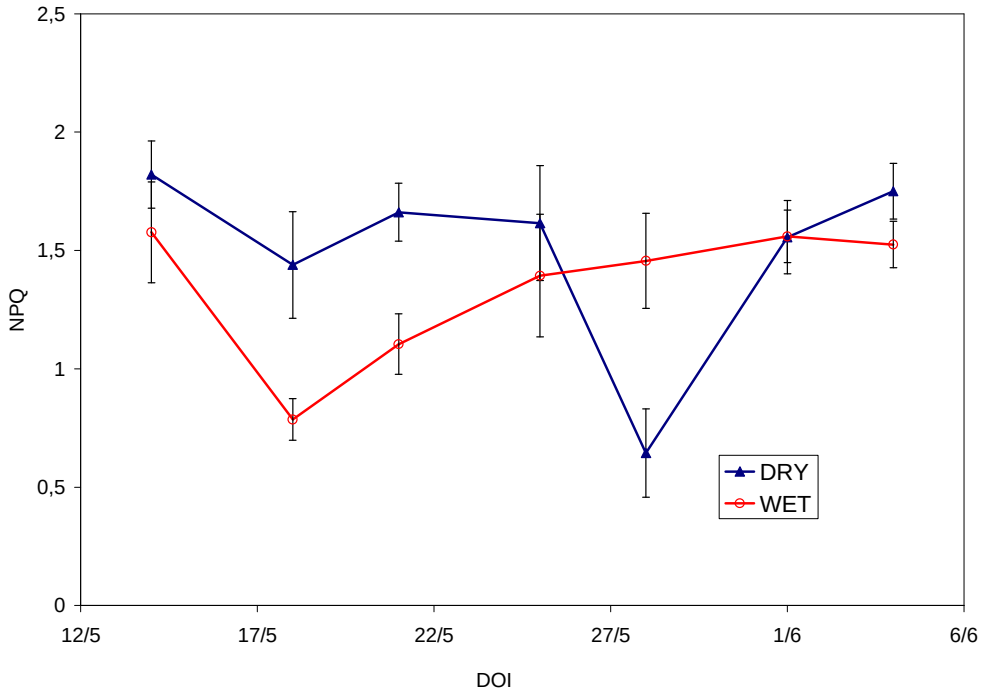

Fig. 18 NPQ of watered and drought stressed plants. Water stress began on 18 May (doi 138) and last until 1 June (doi 152). Each point is the mean of 5 measures. Bars are SEs.

The chlorophyll fluorescence measures of 2005 field experiment consist principally of sampling the PSII maximum efficiency periodically during the stress imposition. The experience of the previous year suggested that this parameter fit better than NPQ for the description of a long-term stress.

The data obtained (Fig. 19) suggested that plants acclimatized to a partially shaded light environment display Fv/Fm values higher than plants kept in full sunlight. Moreover the imposed drought stress caused a fall of PSII maximum efficiency only in the SL treatment (drought stressed in full sunlight) at the end of the experiment.

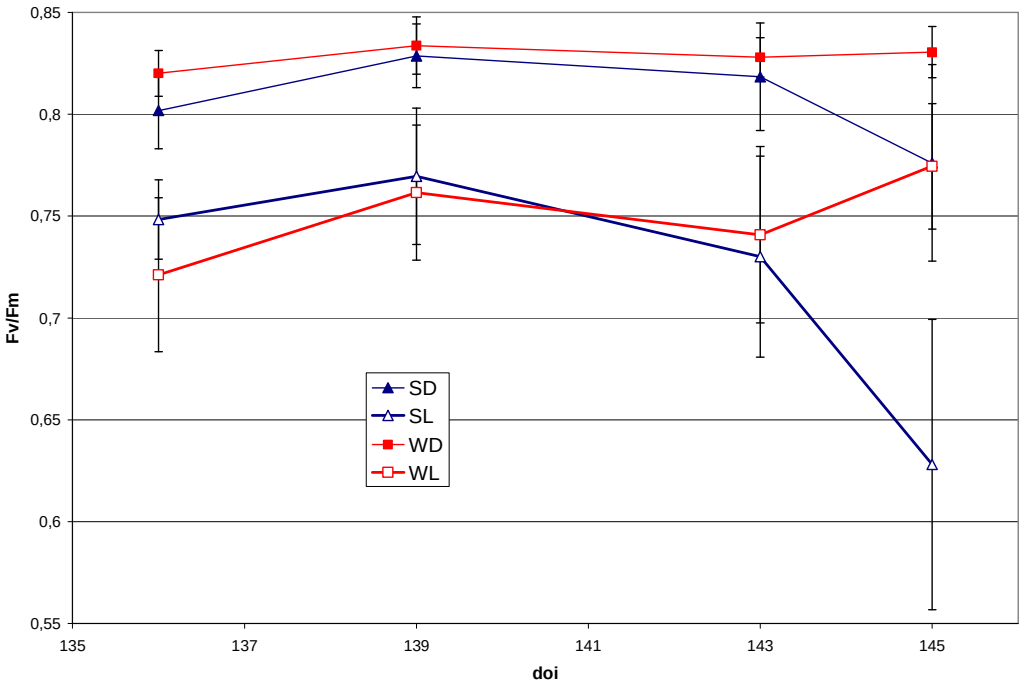

Fig 19 Maximum quantum efficiency of PSII (Fv/Fm). SD: water stressed, dark environment; SL: water stressed, full light; WD: watered, dark environment; WL: watered, full light. Each point is the mean of 5 measures. Bars are SEs. Water stress began on the 16 May (doi 136).

4.2 Short-term stress

4.2.1 VDE gene expression analysis

The indoor short-term light stress allowed us to collect data about the dynamics induced only by light in a tight controlled environment.

VDE gene expression analysis in *Arbutus unedo* showed the highest expression in the leaves immediately before the beginning of the stress and an abrupt decline to non-detectable level of the VDE transcript was registered after ten minutes from light switching on (Fig. 20). After 30 minutes VDE expression was still visible but it remained very low (less than 10% of the initial value) during all the stress period (Fig. 20).

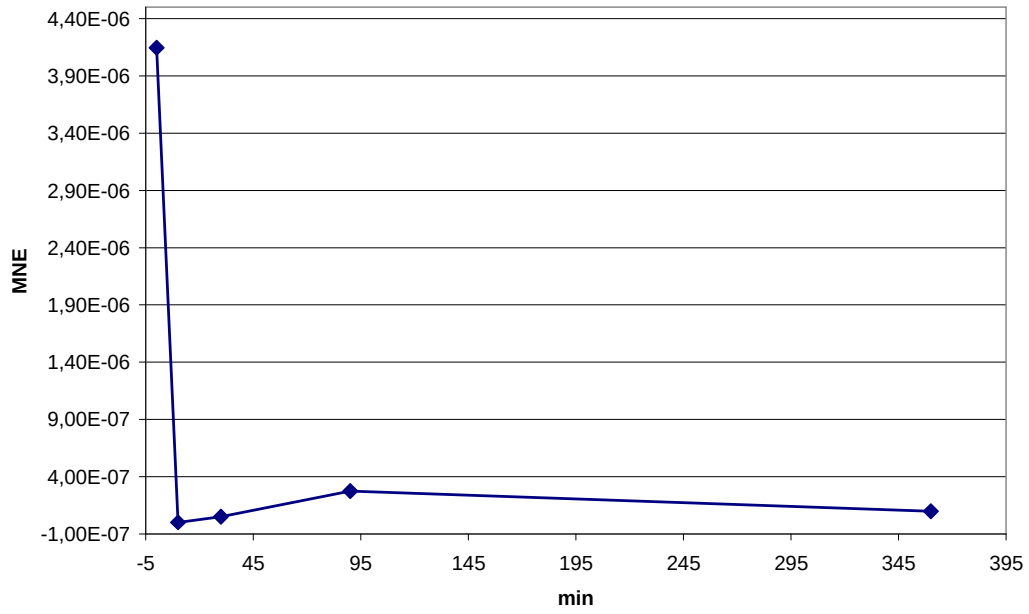

Fig. 20 Mean normalized expression (MNE) of VDE gene in *Arbutus unedo* during a short-term light stress. Values are normalized with 18S gene expression.

Also *Arabidopsis* plants were used for short-term light stress in order to have a useful comparison between two different species.

The main part of the studies on *Arabidopsis* was focused on gene expression and in particular on the different induction of a set of light responsive gene in Col-0 and *cds1-2* plants (also called KD-SOD because they are Knock-Down mutants with a limited expression of SuperOxide

Dismutase). The fifty-six genes chosen and APX2 were previously detected (Bechtold and Mullineaux, unpublished data) as responsive to light stress induced by a photosynthetically active photon flux density (PPFD) five fold higher than the PPFD used during plant growing. In addition to these genes, the expression of violaxanthin de-epoxidase has been also measured to find if there is a direct connection between xanthophyll and water-water cycle.

Considering the threshold of two-fold difference either for up- and down-regulation, only a fraction of these genes (13/56) had a significant variation in KD-SOD plants respect to Col-0 after the light treatment (Tab. 5 and Fig.22).

The analysis conducted on VDE, instead, reveals that this gene was underexpressed in the mutant plants during normal growth condition, and after the light stress the expression was lightly increased. But, following the different level of expression separately in the mutant and in wild type, it could be seen that there is a completely different behaviour respect to the light stress. In fact, KD-SOD plants did not alter their VDE expression level while Col-0 plants showed a significant down-regulation after the light treatment (Fig. 23).

In addition, chlorophyll fluorescence analysis showed a sharp difference between inner and outer leaves (Fig. 24) suggesting different behaviours in light adaptation. Gene expression was measured keeping the outer leaves separated from the inners in a subset of 28 light-responsive genes and sampling the leaves both before and after stress imposition.

With this improved method of analysis, 57% of the tested genes were differentially expressed in the mutant respect to wild type and these differences should be determined by the very low activity of the plastidial SOD and therefore of the water-water cycle.

Tab. 5 Light responsive genes used for gene expression studies in *Col-0* and in *cds1-2*. Expression ratios are the "fold difference" between the mutant and the wild type.

Accession number	Function	Expression ratio
AT3G09640	Ascorbate peroxidase (APX2)	1,0
AT1G76790	O-methyltransferase (catechol) putative	0,8
AT1G35710	leucine-rich repeat (LRR XI) transmembrane protein kinase putative (AtRKL11-7)	0,3
AT1G58270	meprin and TRAF homology domain-containing protein / MATH domain-containing protein	1,0
AT3G09840	cell division cycle protein (CDC48)	0,5
AT3g45970	expansin like	0,8
AT5g61510	quinone oxidoreductase - like protein	0,9
AT5G22060	DnaJ protein, putative	1,3
AT5g03030	DnaJ protein-like	0,5
AT4g24280	heat shock protein cpHsc70-1	0,4
AT4G26160	thioredoxin-like 2	0,8
AT1G07360	RRM-containing RNA-binding protein, putative	1,0
AT4g03430	pre-mRNA splicing factor putative	0,8
AT5G58590	Ran binding protein 1 homolog (RanBP1)	0,7
AT4G35090	catalase 2	0,4
AT5G45870	thaumatin-like protein (PR protein)	0,8
AT1g76880	GT-like trihelix DNA-binding protein, putative	1,0
AT4g28140	DNA-binding protein AP2 domain (RAP2.4) putative	0,8
AAF26770	vacuolor sorting protein 35, putative	1,7
AT1G32230	protein belonging to the (ADP-ribosyl)transferase domain-containing subfamily of WWE	0,9
AT3g03270	universal stress protein (USP) family protein / early nodulin ENOD18 family protein	1,4
AT4G23885	expressed protein	2,0
AT5G10695	expressed protein	0,7
U27698	calreticulin (AtCRTL)	0,9
AT3G02040	SRG3 protein	0,7
AT5g58070	outer membrane lipoprotein - like	1,2
AT1G35140	phosphate-induced (phi-1) protein	1,4
AT4g04020	fibrillin, plastid-lipid associated protein putative	0,4
AT3G22840	early light-induced protein 1	1,8
AT5g25450	ubiquinol-cytochrome-c reductase like protein	0,7
At2g32920	disulfide isomerase putative	0,6
AT1g53540	heat shock protein 17.6	0,8
AT3g23990	heat shock protein 60 mitochondrial chaperonin	0,5

AT4g24280	heat shock protein 70	0,4
AT2g29500	heat shock protein small	0,2
AT3g25230	FK506 binding protein FKBP62 (ROF1)	0,6
AT2G46830	transcription factor MYB-related (CCA1)	0,5
AT4G13770	cytochrome P450 monooxygenase (CYP83)	0,8
AT1G52400	beta-glucosidase homolog (BG1)	0,3
AT5G24770	vegetative storage protein 2 (vsp2)	0,6
AT1G21250	wall-associated kinase 1 (wak1)	0,5
AT1G21270	wall-associated kinase 2 (wak2)	0,6
AT4G21580	Quinone-NADPH oxidoreductase	0,9
AT4G10040	cytochrome c	0,7
AT2G26140	ATP-dependent zinc protease putative; FtsH protease, putative	0,8
AT5G56000	heat shock protein 81.4	0,9
AJ242484	FKBP like protein	1,7
AT1G78380	glutathione transferase	1,4
AT1G14200	C3HC4-type zinc finger protein family	1,1
AT1G52870	peroxisomal membrane protein-related	1,7
AT2G01190	octicosapeptide/Phox/Bem1p (PB1) domain-containing protein	1,3
AT5G64400	At5g09570	0,7
AT4G17460	homeobox-leucine zipper protein-like	2,2
AT2G47730	glutathione transferase 6	0,6
AT3G58680	ethylene-responsive transcriptional coactivator (ER24)	2,3
AT1G30070	SGS domain-containing protein, similar to calcyclin binding protein	0,6

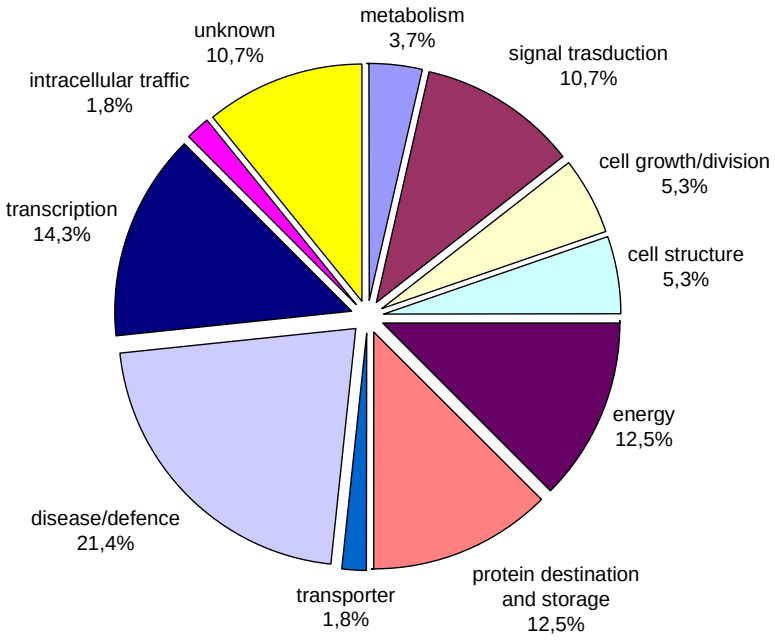

Fig. 21 Functional classification of 56 light stress responsive gene of *Arabidopsis.*

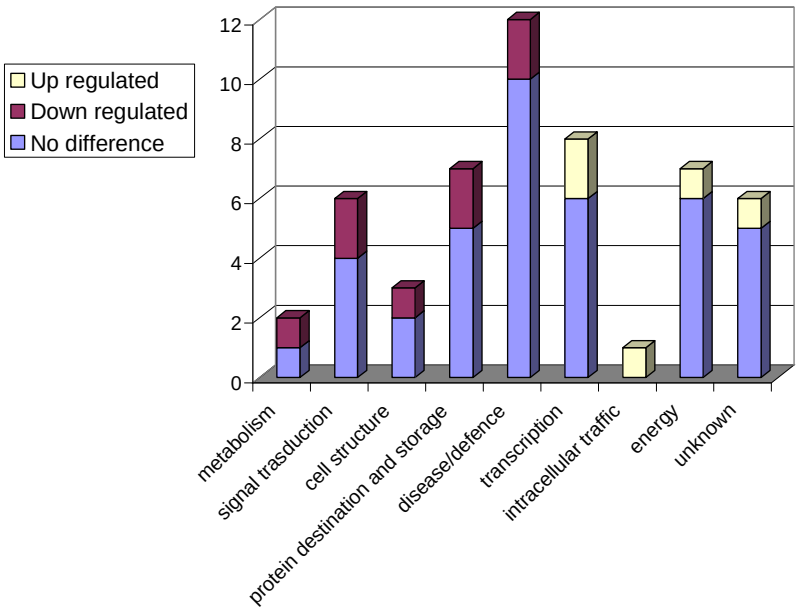

Fig. 22 Functional categorization of light regulated genes in *cds1-2* respect to *Col-0.*

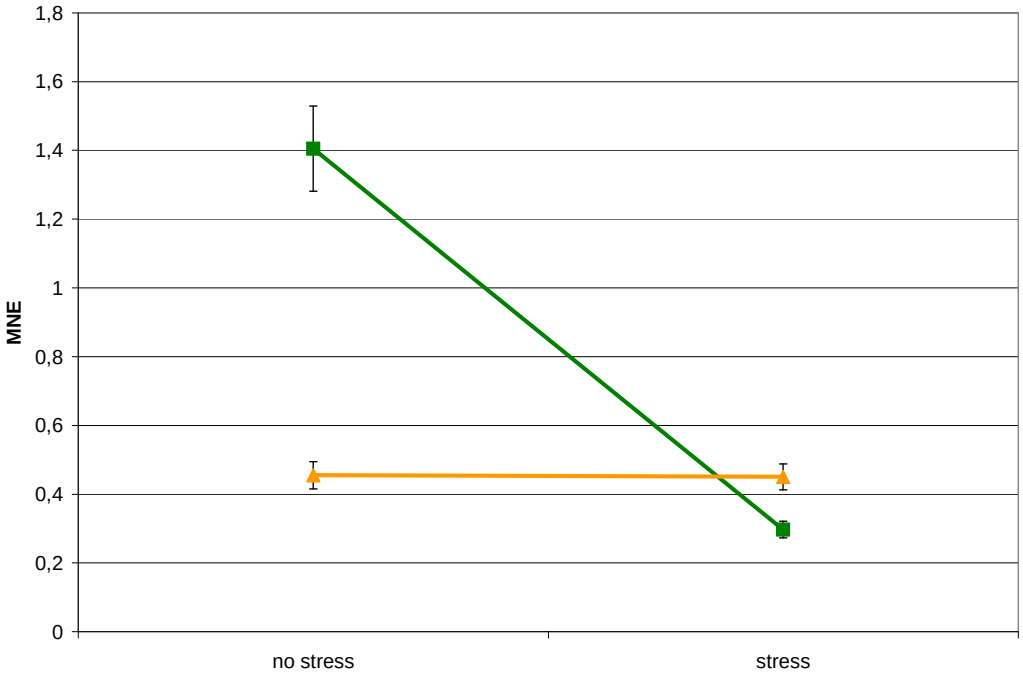

Fig. 23 Expression level of VDE gene in *Arabidopsis* plants immediately before and after the light stress. Col-0 plants are represented by squares, KD SOD plants by triangles. Values are mean±SE (n=2). Expression is normalized using Actin as housekeeping gene.

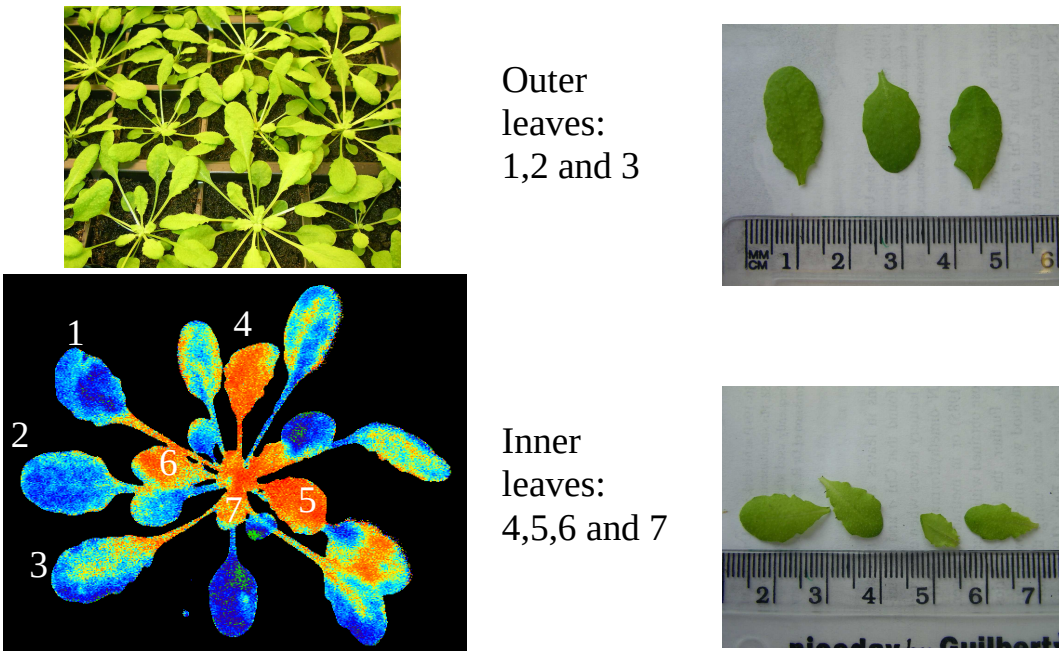

Fig. 24 Differences between inner and outer leaves of *cds1-2* plants. Upper left panel: picture of 7-week old plants. Lower left panel: fluorescence image of a single rosette, the false colours represent different level value of Φ. Right panels: direct size comparison of detached leaves.

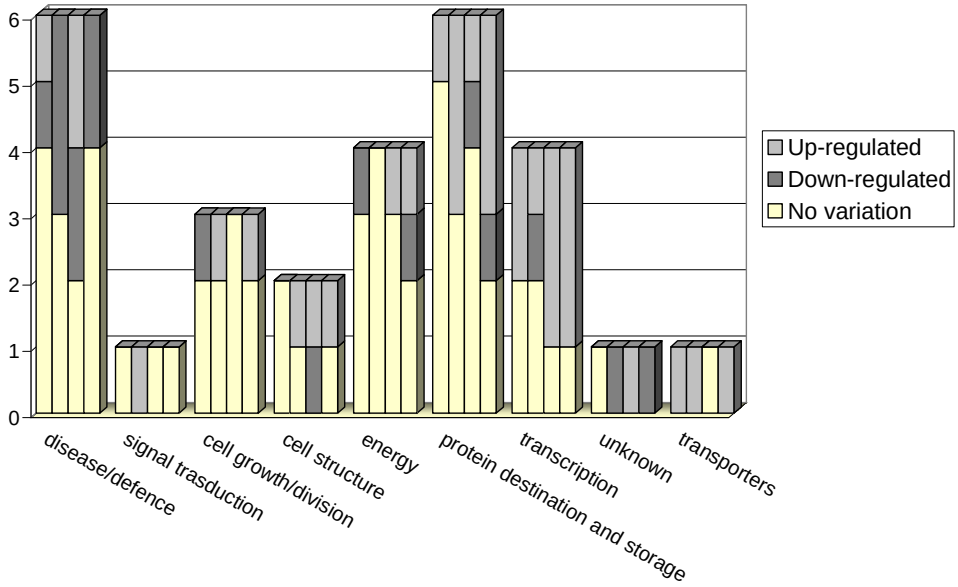

Fig. 25 Functional categorization of light regulated genes in *cds1-2* respect to *Col-0*. The first column of each category represent not stressed inner leaves, the second one is for not stressed outer leaves, the third one is for light stressed inner leave, and the last one is for light stressed outer leaves.

Tab. 6 Light responsive genes studied in inner and outer leaves both before and after stress. Values are expressed as ratios between mutant and wild type plants. In red are underexpressed genes (under the threshold of 0,5) and in green are the up-regulated genes (over the threshold of 2).

Gene Locus	Function	Cds1-2/Col-0			
		Inner leaves No stress	Outer leaves No stress	Inner leaves Stress	Outer leaves Stress
At3g09640	Ascorbate peroxidase (APX2)	1,87	0,23	7,8	0,58
At1g35710	leucine-rich repeat (LRR XI) transmembrane protein kinase putative (AtRKL11-7)	1,6	10,2	1,7	1,2
At1g58270	meprin and TRAF homology domain-containing protein / MATH domain-containing protein, similar to ubiquitin-specific protease 12	0,5	1,0	1,4	1,1
At3g09840	cell division cycle protein (CDC48)	0,9	5,5	0,7	2,6
At3g45970	expansin like	0,9	0,7	3,1	0,9
At5g61510	quinone oxidoreductase - like protein	0,9	1,5	1,0	1,6
At5g22060	DnaJ protein, putative	0,6	1,4	2,4	3,3
At5g03030	DnaJ protein-like	1,3	3,2	0,7	1,4
At4g24280	heat shock protein cpHsc70-1	0,7	2,0	0,6	4,2
At4g03430	pre-mRNA splicing factor putative	2,4	1,4	5,2	2,8
At5g58590	Ran binding protein 1 homolog (RanBP1)	1,7	0,9	1,1	0,6
At1g76880	GT-like trihelix DNA-binding protein, putative	1,8	1,0	4,5	2,3
At4g28140	DNA-binding protein AP2 domain (RAP2.4) putative	8,5	14,1	8,7	1,1
At1g32230	protein belonging to the (ADP-ribosyl)transferase domain-containing subfamily of WWE protein-protein interaction domain protein family.	1,6	1,5	1,5	0,8
At3g03270	universal stress protein (USP) family protein / early nodulin ENOD18 family protein, contains Pfam profile	1,2	0,8	1,8	1,5
At5g58070	outer membrane lipoprotein - like	2,8	2,9	1,7	2,9
At1g35140	phosphate-induced (phi-1) protein	0,8	0,4	17,1	0,2
At4g04020	fibrillin, plastid-lipid associated protein putative	1,6	3,9	0,5	2,3
At3g22840	early light-induced protein 1	1,1	1,1	0,7	5,4
At5g25450	ubiquinol-cytochrome-c reductase	0,4	0,7	5,2	0,1
At2g32920	disulfide isomerase putative	1,7	0,8	1,1	0,9
At1g53540	heat shock protein 17.6	0,1	0,0	0,1	0,3
At3g23990	heat shock protein 60 mitochondrial chaperonin	3,1	0,8	0,9	5,6
At3g12580	heat shock protein 70	1,3	1,1	0,3	0,2
At5g52640	heat shock protein 83	0,9	0,4	2,3	1,8
At2g29500	heat shock protein small	2,5	0,9	0,4	0,1
At3g25230	FK506 binding protein FKBP62 (ROF1)	1,2	3,4	1,2	1,2
At2g46830	transcription factor MYB-related (CCA1)	0,7	0,3	0,7	2,5

4.2.2 Chlorophyll fluorescence analysis

Short-term light stress gave data about the dynamics induced only by light in a tight controlled environment. As in the field experiment, in *Arbutus* plants, the light caused a rapid drop in the efficiency values largely caused by a decline of F'm values (Fig. 26).

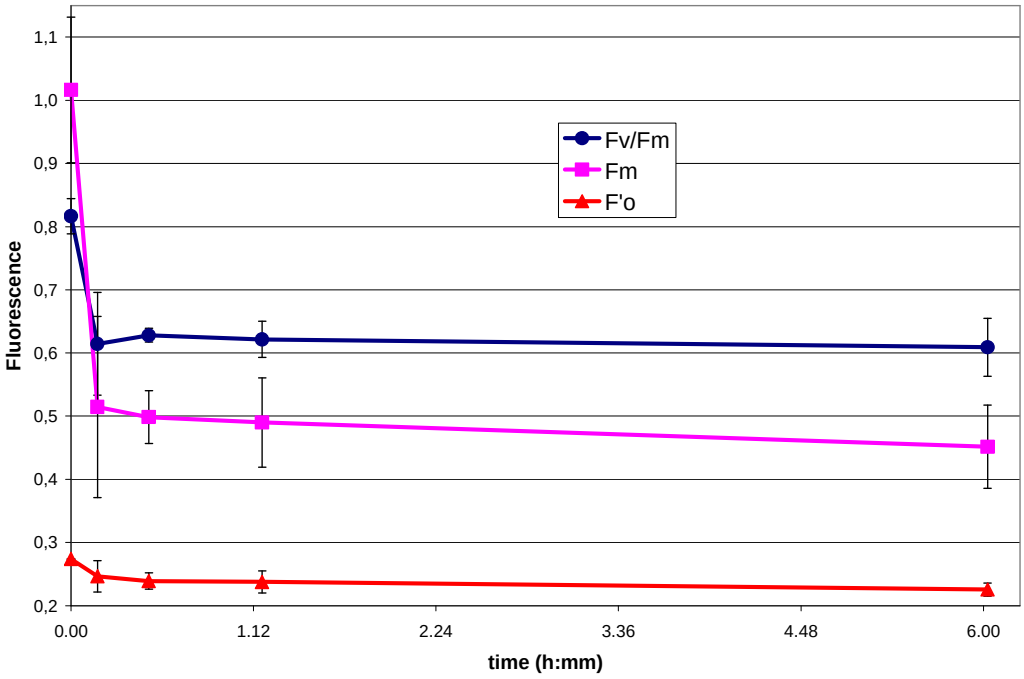

Fig. 26 Chlorophyll fluorescence parameter Fv/Fm (or Fq'/Fm'), F'm and F'o. Plants were subjected to a 6h light stress as described in materials and methods. Points are means of two samples ± SE.

NPQ values were also calculated and it could be seen that after the fast raise caused by the beginning of light imposition, there was a transient drop and a following constant increase (Fig. 27)

After the light stress period, the lamps were switched off and fluorescence values were recorded for the following twenty-four hours with the plants in a completely dark environment. As found in the field experiment, the recovery of the PSII maximum efficiency was not complete after 8-10 hours and it took about twenty hours to be fully restored (Fig. 28).

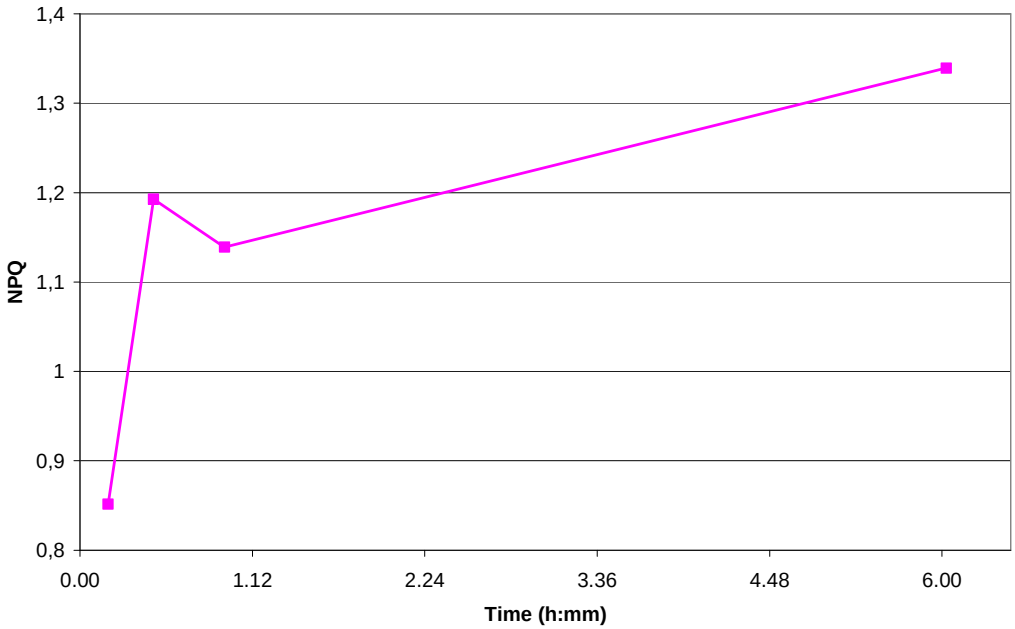

Fig. 27 Non Photochemical quenching (NPQ) of *Arbutus* leaves exposed to saturating light. Points are means of two samples ± SE. For point lacking error bars the SE was smaller than the symbol size.

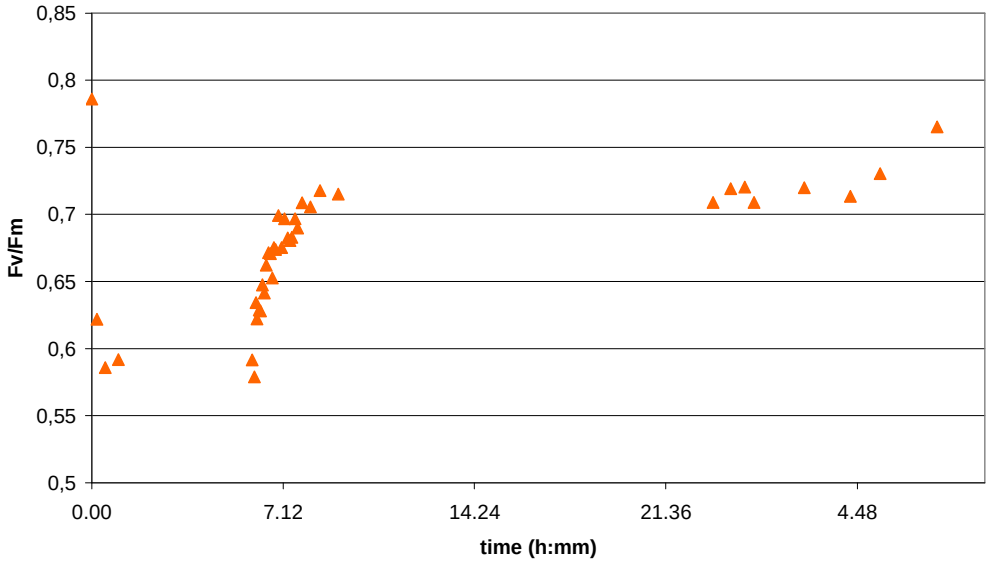

Fig. 28 *Arbutus* maximum quantum efficiency of PSII (Fv/Fm) during the light stress period followed by 24 hours of dark.

In *Arabidopsis*, chlorophyll fluorescence measure, both before and after light stress, displayed that the mean value of the rosettes are the same in mutant and wild type (Fig. 29). On the contrary, in the KD-SOD plants the

images obtained from the Fluorimager showed main differences between inner and outer leaves (Fig. 24)

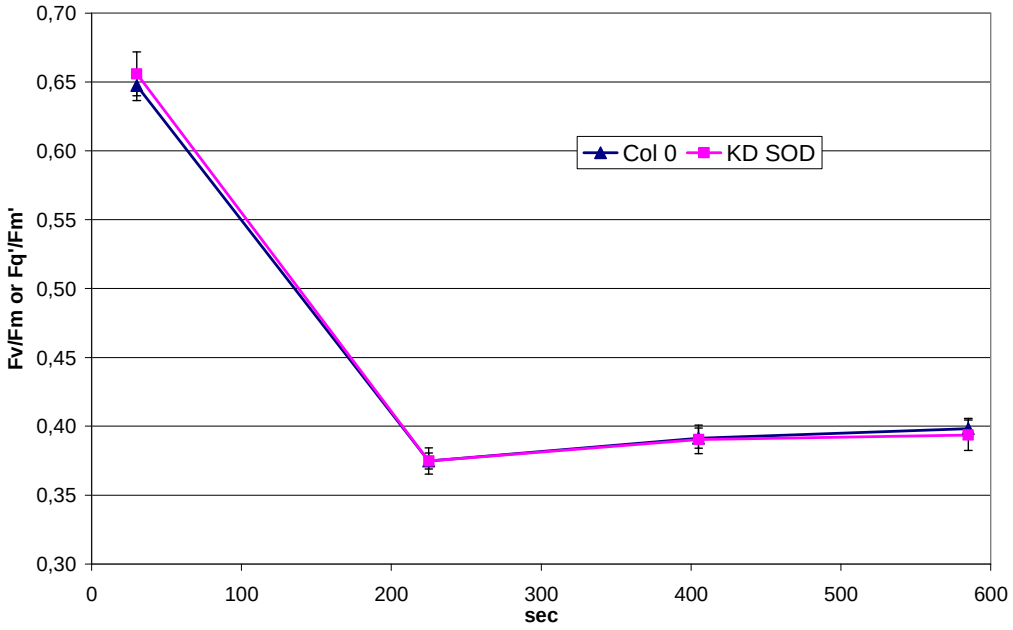

Fig. 29 Fv/Fm of Fq'/Fm' values of *Arabidopsis* rosettes after one hour under saturating light. Points are the mean of ten values ±SE.

4.2.3 ROS Imaging and quantification

In order to find the cause of the lack of an expression regulator system in the *Arabidopsis cds1-2* mutant, an altered ROS content was searched due to the deprived enzymatic activity of the plastidial SOD.

The altered level of superoxide was the main difference seen: the wild type plants had higher concentration of this ROS after the light stress than the mutant. Moreover, *cds1-2* plants did not have any significant variation in superoxide content (Fig. 30).

Under the growth condition used, *csd1-2* plants had paler leaves in the centre of the rosette compared with wild type, but these leaves attained almost a normal appearance as they matured. This visible phenotype was reflected in significant differences in chlorophyll content between mutant and wild type plants (Fig. 34).

Hydrogen peroxide content assays in the leaves were conducted in order to find out other diversities in oxygen metabolism between the two varieties of

Arabidopsis plants. Inner and outer leaves were maintained separated but no significant diversity in H_2O_2 was found (Fig. 31).

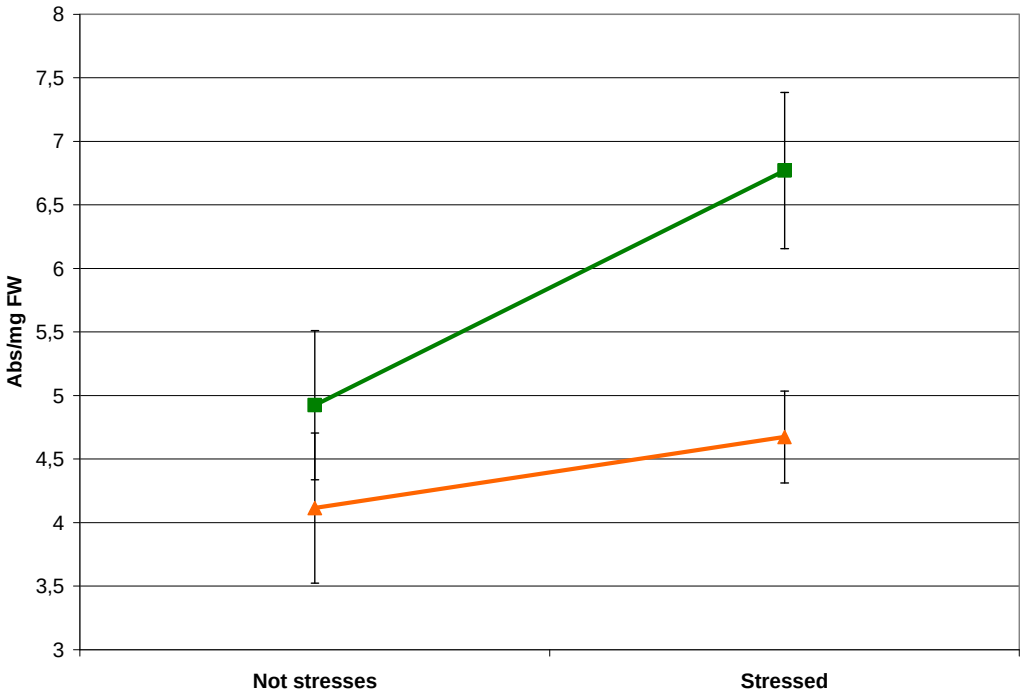

Fig. 30 Superoxide content measured colorimetrically on leaf extract. Col-0 plants are represented by squares, KD SOD plants by triangles. Points are means ± SE of six samples.

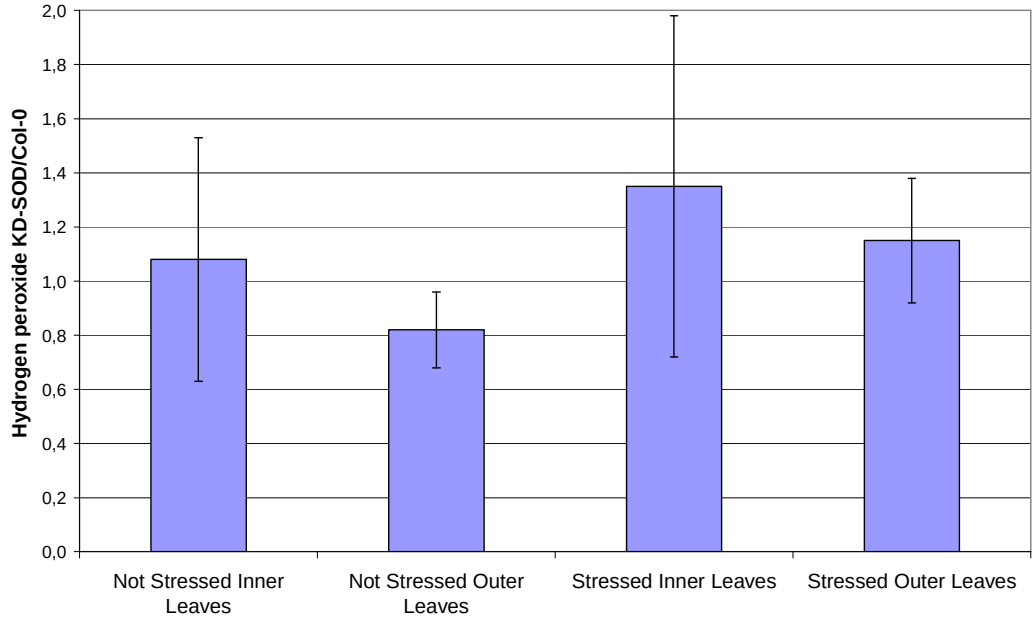

Fig. 31 Hydrogen peroxide content expressed as ratio between mutant and wild type.

The images used for ROS localisation were obtained sampling the larger leaves of each rosette. So the results should be considered as referred to outer leaves.

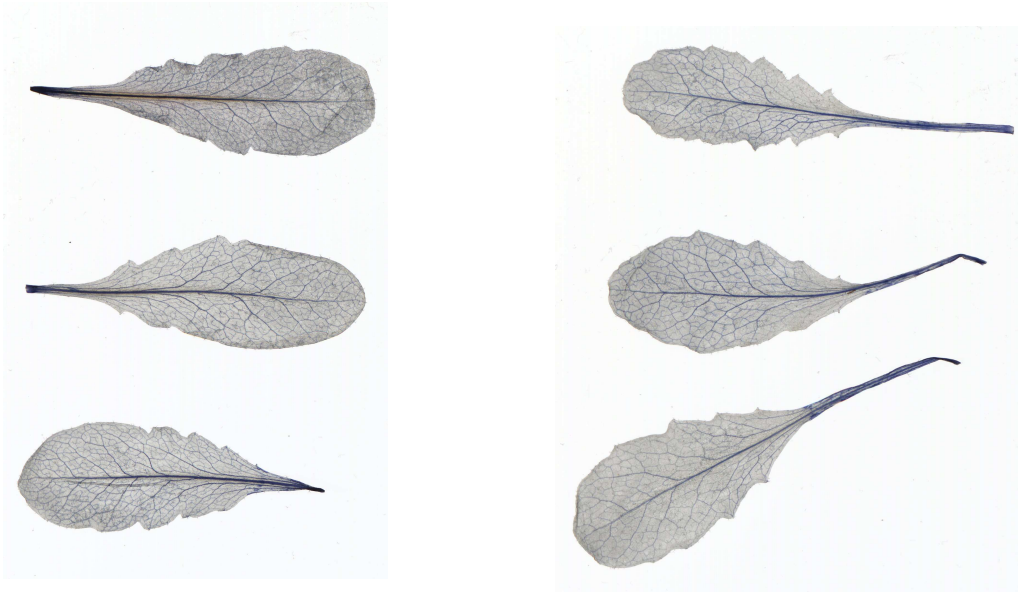

Fig. 32 NBT stained leaves. On the left there are KD SOD leaves and on the right the wild type leaves

ROS distributions inside leaf tissues were very similar (Fig. 32 and 33) and even the used software for image analysis (ImageJ) found that the distribution pattern of the dyes are very close to each other (data not shown).

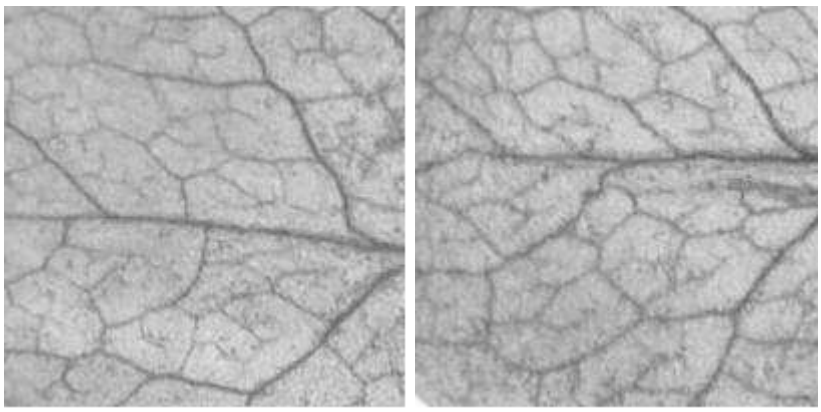

Figura 33 Magnification of NBT stained leaf lamina**.** The left panel is the mutant, the right one the wild type.

The differences between KD-SOD and wild type were limited to the outer leaves where, as previously seen, a lower content of superoxide after the treatment, and a smaller presence of hydrogen peroxide before the light stress were detected.

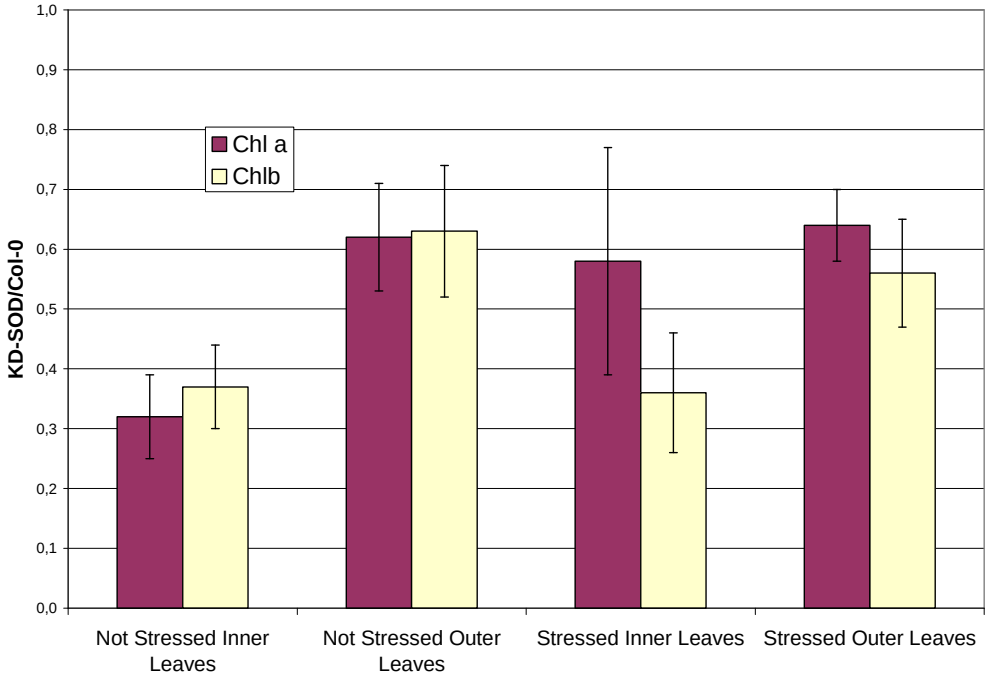

Fig. 34 Chlorophyll content of *cds1-2* plants compared to *Col-0*. Analysis was conducted keeping the inner leaves separated from the outer and the measures were repeated both before and after stress imposition.

4.2.4 Xanthophyll analysis

Arbutus leaves exposed to the short-term light stress showed a rapid raise of DEPS in the first minutes of the experiment. Then a transitory decline followed by a second slow increase was observed (Fig. 35).

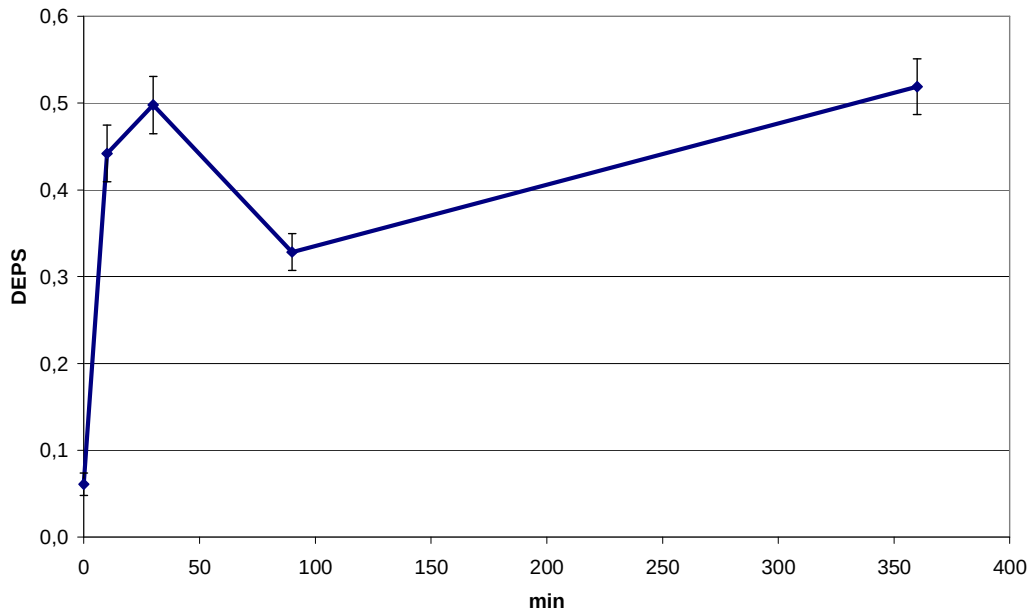

Fig. 35 DEPS values of *Arbutus* leaves exposed to saturating light. Points are means of two samples ± SE

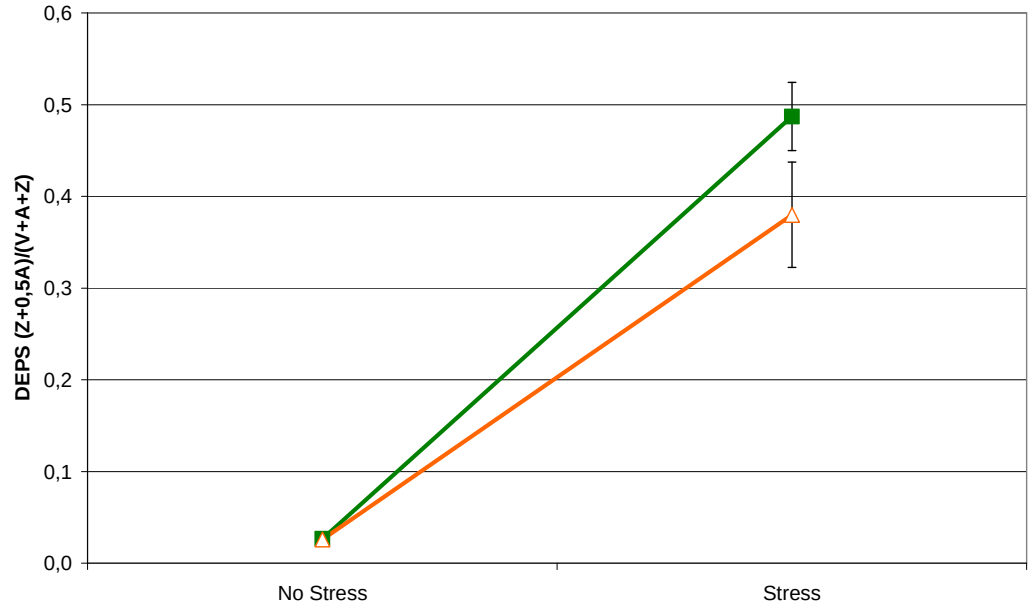

Fig. 36 DEPS values of *Arabidopsis* leaves exposed to saturating light for one hour. Col0 plants are represented by squares, KD SOD by triangles. Points are means of two samples ± SE

De-epoxidation state was also measured in *Arabidopsis* leaves belonging to Col-0 and *cds1-2*. As expected after light stress imposition DEPS values increased but no significant difference appeared between wild type and mutant plants (Fig. 36).

5.Discussion

5.1 Long-term stress

Water deficit, generally associated with high solar irradiation and high temperatures during the summer, has been considered the main limiting factor for plant growth in Mediterranean-type ecosystem. *Arbutus unedo* is an evergreen shrub or small tree that grows in young oak forest and developing woodland, rocky places in the Mediterranean region, and displays several mechanisms of drought stress resistance. The present study was aimed at better understanding of the response of this species to drought stress, the relationship between chlorophyll fluorescence, xanthophyll content and VDE gene expression in leaves was emphasized.

The chlorophyll fluorescence studies showed that high irradiance and drought affected PSII efficiency. During the stress period, PSII maximum efficiency decreased in a non-linear way: in the first part of the stress period, the loss of efficiency was modest but in the last days of drought, this deficit became substantial (Fig.10 and 15). Nevertheless, the first field experiment showed that, even after two weeks of drought, *A. unedo* plants were able to recover completely their photosynthetic capacities.

Zeaxanthin dependent quenching was the main cause of this loss in efficiency but sustained damages to the protein complex of the photosystems could have a noteworthy role in this process. In order to discern the different contributes to this loss in PSII maximum efficiency, we correlated DEPS and Fv/Fm values.

Three of the four treatments of the second long-term stress experiment (SD, WL and WD) showed a strong negative correlation (R^2>0,9) between the maximum efficiency of PSII and the conversion state of xanthophylls (Fig 37). Moreover the equations derived from these relationship have a y-intercept close of 0,85 that is the value near to the optimal value for non-stressed plant measured for most plant species (Maxwell & Johnson 2000) and even for *A. unedo* (Fig. 19). These relationships denote that most of the

variation of PSII maximum efficiency is caused by the presence of zeaxanthin in the leaves, even before dawn.

Plants under full light and water stressed (SL), instead, show a different relationship between Fv/Fm and DEPS with a R^2 value below 0,8 and a y-intercept of 0,9. However, it could be seen that only one point, corresponding to the night of highest stress, is far from the line that intersect the other three points. If we exclude this point from the regression, again we obtain a strong negative correlation (R^2= 0 ,95) and a y-intercept that correspond to the PSII maximum efficiency of non stressed plants (Fig. 38).

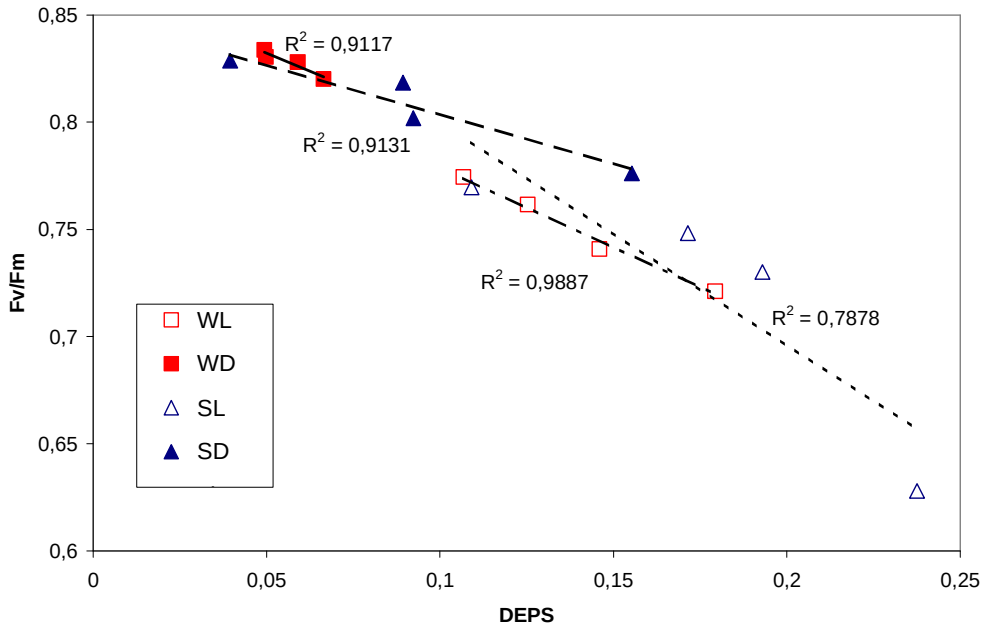

Fig. 37 Relationship between PSII maximum efficiency and de-epoxidation state of xanthophylls. Samples collected from watered plants are denoted by squares while triangles are for water stressed plants. Open and solid symbols represent plants under full sunlight and partially shaded respectively. Data from Fig 15 and 19.

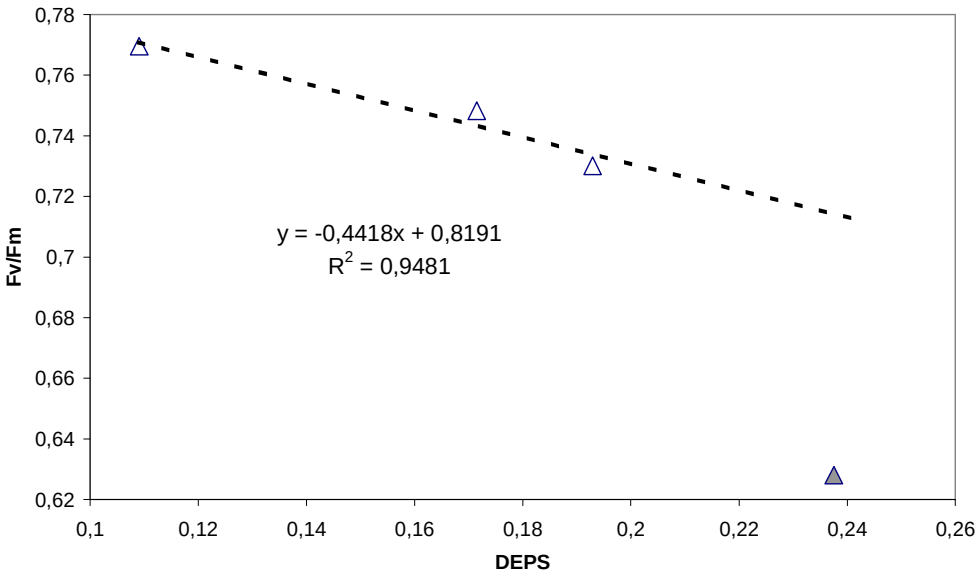

Fig. 38 Relationship between PSII maximum efficiency and de-epoxidation state of xanthophylls of the Stressed-Light treatment. The linear regression of the first three points is shown. See text for details.

Therefore, de-epoxidation state of xanthophylls can explain the variation in PSII maximum efficiency with the exception of the point of highest stress, when probably a sustained photo-damage occurred.

Our experience suggested that some chlorophyll fluorescence parameters were better than others to follow long-term stress physiology. NPQ was not useful to measure stress response because it soon fail to work due to zeaxanthin night retention. In fact, maximum fluorescence values recorded pre-dawn were already non-photochemically quenched few days after the beginning of the drought period and the measure lost its prerequisite to be relative to a non-stressed dark adapted state (Maxwell & Johnson 2000). To avoid this problem, a periodic measure of PSII maximum efficiency throughout the experiment had to be preferred to quantify the stress conditions of photosystems caused by the combination of drought and high irradiance.

As previously reported (Munne-Bosch & Penuelas 2004), in *Arbutus unedo* the total amount of xanthophyll remains unaltered under moderate stress. Our data suggest that plants fully exposed to sunlight displayed a higher

concentration of xanthophylls per chlorophyll unit than shaded plants and these ratios remain almost constant throughout the experiment (Fig. 14). Therefore, *A. unedo* plants seem to regulate total xanthophyll content responding to light regimes more than to water status.

However that proportions of zeaxanthin and violaxanthin were largely altered by the water-stress treatment (Fig. 15).

Zeaxanthin is present inside leaves at higher concentration when thermal dissipation is needed to protect the photosynthetic apparatus from the excess of energy (Congming et al. 2003;Demmig et al. 1987;Demmig-Adams et al. 2006), so leaves fully exposed to sunlight have, at midday, the highest zeaxanthin content. Even shaded leaves show high DEPS values when water is not available (Fig. 17). In fact, the imbalance between the activity of the photosystems and the electrons required for photosynthesis, principally caused by stomatal closure, lead to an over-excitation that had to be dissipated to avoid damages.

Moreover, a considerable retention of zeaxanthin and antheraxanthin at night is visible during the experiment in both the treatments with water-stressed plants (Fig. 15). The incomplete epoxidation of xanthophyll was previously reported in response to different environmental stresses (Congming et al. 2003;Demmig-Adams et al. 2006;Ebbert et al. 2005;Gilmore 1997;Latowski, Grzyb, & Strzalka 2004;Verhoeven, Demmig-Adams, & Adams III 1997) when a rapid induction of thermal energy dissipation is necessary during morning. In fact, during our experiment the plants subjected to a prolonged period of water shortage were forced to increase energy dissipation from the first hours of the day to avoid photo-damage.

Despite extensive analysis of the xanthophyll cycle at the biochemical and biophysical level, little is understood about the regulation of the genes involved. In fact, no molecular genetic studies have been undertaken to understand the contribution of xanthophyll cycle gene expression to the photo-protective response in mature plants during field experiments.

Although it has been established that violaxanthin de-epoxidase activity is stimulated by the lumen acidification that occur in excess light conditions it is possible that the diurnal changes observed in violaxanthin and zeaxanthin result not only from post-translational regulation of VDE activity, but could involve change in RNA and protein expression level.

Analysis of expression during chloroplast differentiation has shown that the VDE gene is induced by white light illumination (Woitsch & Romer 2003) and during leaf development VDE transcript abundance were found to vary, with levels increasing as leaves matured (Bugos, Chang, & Yamamoto 1999). These works did not explain the mechanisms that control VDE gene expression but show a peculiarity that emerge also from our data: the timing of the peak of expression did not correlate directly with the periods of maximal activity of the enzyme.

Our data showed unequivocally that VDE gene expression have the highest values during the night (Fig. 13) when no activity of the enzyme would be expected. This opposite pattern between transcript abundance and physiological requirement could be partially explained with an anticipated protein synthesis to compensate diurnal enzyme degradation. Supplementary data about VDE gene expression in *Arbutus* came from the short-term stress and will be discussed later in the text.

During the experiment, a general decrease of VDE gene transcript abundance in drought-stressed plant was also visible (Fig. 13). This decrement could be due to a co-ordinate regulation of gene with photosynthetic function. As previously mentioned, the reduction of stomatal conductance to decrease transpiration also limits the entry of CO_2 into leaves, which causes previously non-saturating light intensities to become in excess of photosynthetic capacity. The reduction of photosynthesis by decreasing production of photosystem complexes and associated pigment could thus be achieved in part by reducing transcript steady-state levels. Previous work on *Arbutus* (Baraldi et al. submitted) reported a 30% decrease of chlorophyll pigment in drought-stressed plants and our data show that the foliar ratio between xanthophyll and chlorophyll

concentration is stable. Therefore, it could be hypothesised that the reduced xanthophyll pool needs a smaller gene expression of the enzymes for their conversion. The factors that cause the increase of VDE gene expression during the experiment in watered plants under full sunlight (WL) plants remain to be clarified.

Our VDE expression studies suffered the presence of two imperfection: the measure of gene expression were derived from leaves that are near but different from the ones used for xanthophyll content essay and the high costs of these analysis made impossible to manage a large sampling group.

Although these problems, it was obtained a physiological picture that contain many noteworthy link between xanthophyll content, VDE gene expression and chlorophyll fluorescence parameters.

5.2 Short-term stress

In actively photosynthesising leaves, sudden changes in environmental conditions, such as an increase in light intensity, can result in an increase in excitation energy in excess respect to that required for photosynthetic metabolism (Asada 1999;Bechtold, Karpinski, & Mullineaux 2005;Long, Humphries, & Falkowski 1994;Mullineaux & Karpinski 2002). To deal with excess excitation energy, plants have developed efficient mechanisms for its thermal dissipation in order to protect the photosynthetic apparatus from damage (Niyogi 1999).

However, in many situations quenching of excess excitation energy by such mechanisms cannot prevent over-reduction of components of the electron transport chain (Foyer & Mullineaux 1998). Under such conditions chlorophyll triplet states form in photosystem II (PSII) and react with oxygen to form singlet oxygen ($^1O_2$), which leads to PSII reaction centre damage and increased rates of lipid peroxidation (Hideg et al. 2002;Krieger-Liszkay 2005;Kruk et al. 2005;Montillet et al. 2004).

Photochemical quenching processes also dissipate excess excitation energy by diverting electrons into metabolic sinks other than primary metabolism,

preventing over-reduction of the PSII electron acceptors (Asada 1999;Ort & Baker 2002). Exposure to light levels considerably in excess of those required to saturate carbon metabolism, can result in increased rates of electron transport in the absence of any increase in CO_2 assimilation. Under such conditions, O_2 is a prominent candidate for an alternative electron acceptor to CO_2 (Asada 1999;Ort et al. 2002). O_2 can be photo-reduced by PSI to produce superoxide anion radicals ($O_2^{\cdot -}$), which are rapidly converted to hydrogen peroxide (H_2O_2) by superoxide dismutase(Asada 1999).

Our short-term light stress experiment was carried out to investigate these processes and to integrate the dataset of the long-term experiments with the fast response dynamics expressed by plants to deal with the "sudden changes in environmental" condition previously mentioned.

In addition to *Arbutus unedo*, the experiment was conducted also on *Arabidopsis thaliana* to take advantages both from the huge knowledge on its genetic and from mutant availability (i.e. *cds 1-2*).

Pigment composition data (Fig. 35 and 36) showed that both *Arabidopsis* and *Arbutus* display an immediate raise in the de-epoxidation state of xanthophylls caused by the light stress.

Close correlation have been found between zeaxanthin and antheraxanthin contents and NPQ in different plant species under a wide range of environmental conditions (Adams et al. 2002;Demmig-Adams et al. 2006) and also our data showed that DEPS and NPQ followed the same pattern during the stress imposition both in *Arbutus* and *Arabidopsis* (Fig. 39 and Fig. 40).

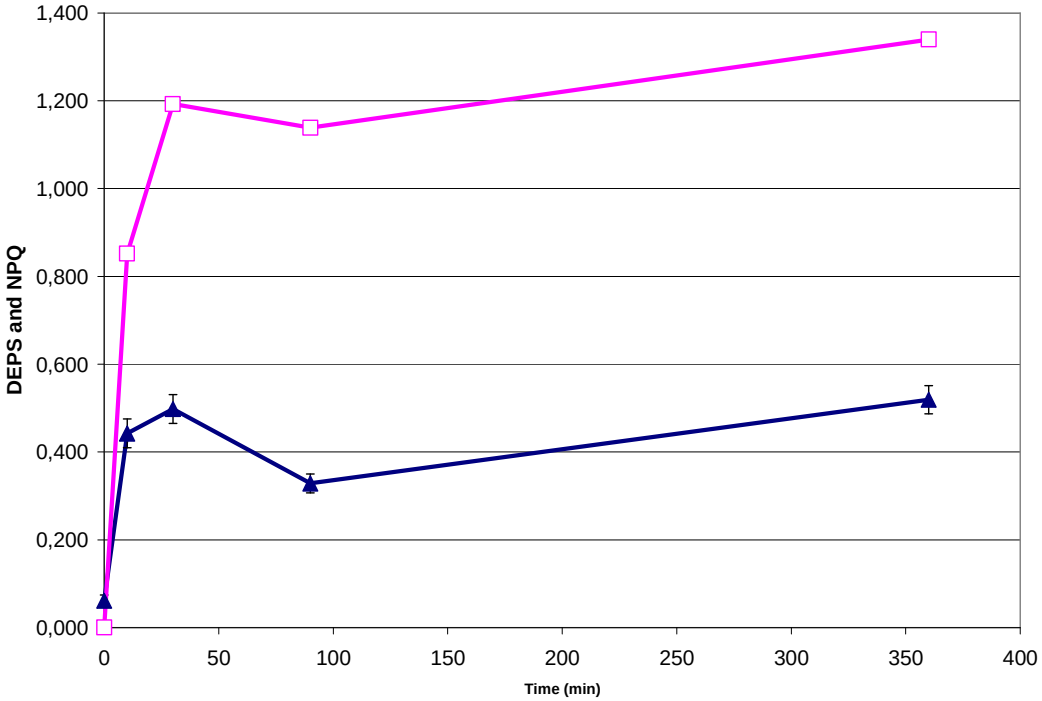

Fig. 39 Trends of DEPS and NPQ during short-term light stress in *Arbutus* plants. DEPS values are indicated with solid triangles and NPQ values with open squares. Each point is the mean of two values and bars are SEs. For point lacking error bars the SE was smaller than the symbol size. Data from Fig. 27 and 35.

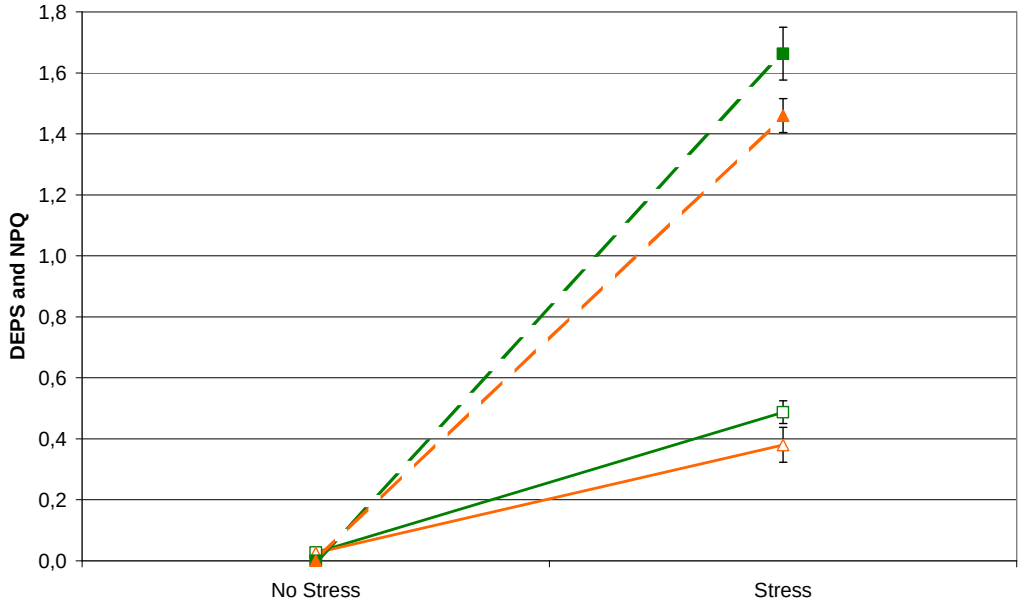

Fig. 40 Trends of DEPS (solid lines) and NPQ (dashed lines) during short-term light stress in *Arabidopsis*. Col-0 plants are represented by squares, KD SOD plants by triangles. Each point is the mean of two values and bars are SEs. For point lacking error bars the SE was smaller than the symbol size. Data from Fig. 36.

In addition, we observed that DEPS and NPQ values of the two different *Arabidopsis* genotype (Col-0 and KD SOD) did not show any significant difference. This means that also the KD-SOD plants need xanthophyll-based dissipation process to deal with high light environment in spite of the reduced amount of chlorophyll (Fig. 34) present in their leaves.

The de-epoxidation state and the non-photochemical quenching of *Arbutus* had a rapid increase from the beginning of the stress to the second sampling point (30 minutes) and then a transient drop and a following rise until the end of the experiment were visible. This transient decrement indicates a conversion of zeaxanthin back to violaxanthin also during excess light stress although for a limited extent. It is not known if this behaviour is caused by a variation of stromal pH that avoid VDE activity or by any other physiological variation inside chloroplast. However comparing DEPS (or NPQ) and VDE gene expression level a clear relationship results (Fig. 41).

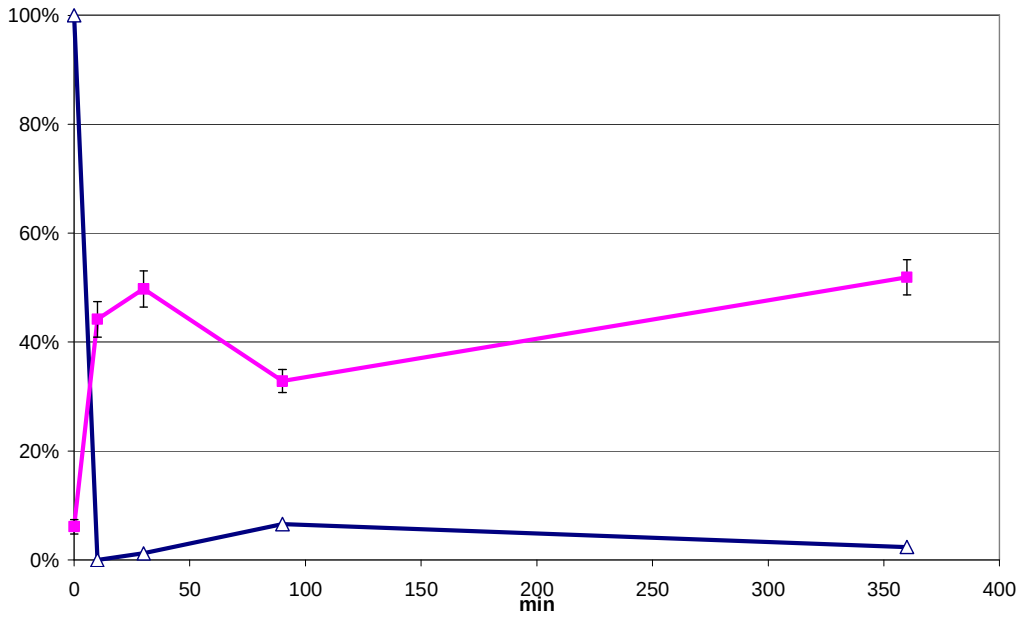

Fig. 41 VDE expression and DEPS level during short term stress in *Arbutus*. DEPS values are indicated with solid squares and VDE gene expression values (MNE) with open triangles. Each point is the mean of two values and bars are SEs. For point lacking error bars the SE was smaller than the symbol size. Data from Fig. 20 and 35.

These data could suggest that light regimes control VDE transcript abundance through xanthophyll de-epoxidation state. Moreover, in the long-term stress, the same dynamics occurred (Fig. 13 and 15): during the days, the high values of zeaxanthin lowered VDE expression while, during the nights, a lesser amount of the de-epoxidated xanthophylls allowed the expression of VDE gene.

Arabidopsis Col-0 plants, like *Arbutus*, showed a fall in VDE expression in correspondence with the rise of DEPS values caused by light stress (Fig.23). KD-SOD mutants, instead, had a constant level of VDE expression that is coincident with the level of the treated Col-0 despite the variation in DEPS values.

This could be an evidence that VDE gene expression is subordinate to some second factor that repress transcription during the dark period and that there is a relationship between water-water and xanthophyll cycles. In fact, a reduced activity of the first cycle brings to a modified induction of the enzymes of the second one.

In addition, it was observed that in the mutant plants lack the increase of superoxide visible in the wild-types (Fig. 30), while the quantity and distribution of the main activated oxygen species remain nearly unaltered (Fig. 31 and Fig. 33).

This could be caused by the smaller amount of chlorophylls that in KD SOD plants reacts with light (Fig. 34) respect to wild-type plants or by the overall alteration of gene concerning ROS metabolism that was previously reported (Rizhsky, Liang, & Mittler 2003). The mutation in KD SOD plants, in fact, concerns the Mehler reaction that has been proposed to be a major source of chloroplastic H_2O_2 (Asada 1999;Ort et al. 2002). Under stress conditions this source of H_2O_2 has been suggested to be a signal for gene expression in response to environmental stress (Chang et al. 2004;Fryer et al. 2003;Mullineaux et al. 2002).

The changed transcript levels of 23/28 genes in the *csd2-1* mutant compared with wild-type plants (Tab. 6) does support the notion that H_2O_2 sourced from the chloroplast may be part of a signalling system regulating

the expression of the majority of EL-responsive genes both during leaf development and under excess light stress.

It is noteworthy that APX2 is among the genes whose expression is affected by the csd2-1 mutation (Tab. 6), suggesting that a chloroplast-source of ROS may be important in the regulation of expression of this gene as was previously proposed (Fryer et al. 2003). However, interpretation of these data should be treated with caution for at least three reasons, none of which are mutually exclusive. First, *csd2-1* still has ca. 40% of CSD2 present (Rizhsky, Liang, & Mittler 2003). Second, there may be redundancy in cells in the production of H_2O_2 derived from $O_2^{\cdot -}$ generated by the Mehler reaction. For example, FSD1 (At4g25100) coding for stromal Fe-SOD has been shown to have partly increased expression in *csd2-1* under non-stress conditions (Rizhsky et al. 2003). Finally and to our knowledge, nothing is known about the tissue specificity of CSD2 expression and therefore it remains possible that the *csd2-1* phenotype is not manifested in some tissue simply because the gene does not express there.

Reference list

1. Adams W.W. et al. (2002) Photosynthesis and photoprotection in overwintering plants. *Plant Biology* **4**, 545-557.

2. Apel K. & Hirt H. (2004) REACTIVE OXYGEN SPECIES: Metabolism, Oxidative Stress, and Signal Transduction. *Annu.Rev.Plant Biol.* **55**, 373-399.

3. Arora A., Sairam R.K., & Srivastava G.C. (2002) Oxidative stress and antioxidative system in plants. *Current Science* **82**, 1227-1238.

4. Asada K. (1999) THE WATER-WATER CYCLE IN CHLOROPLASTS: Scavenging of Active Oxygens and Dissipation of Excess Photons. *Annu.Rev.Plant Physiol Plant Mol.Biol.* **50**, 601-639.

5. Asada K. (2006) Production and scavenging of reactive oxygen species in chloroplasts and their functions. *PLANT PHYSIOLOGY* **141**, 391-396.

6. Aspinall-O'Dea M. et al. (2002) In vitro reconstitution of the activated zeaxanthin state associated with energy dissipation in plants. *Proc.Natl.Acad.Sci.U.S.A* **99**, 16331-16335.

7. Badger M.R. et al. (2000) Electron flow to oxygen in higher plants and algae: rates and control of direct photoreduction (Mehler reaction) and rubisco oxygenase. *Philos.Trans.R.Soc.Lond B Biol.Sci.* **355**, 1433-1446.

8. Baker N.R. et al. (2001) High resolution imaging of photosynthetic activities of tissues, cells and chloroplasts in leaves. *Journal of Experimental Botany* **52**, 615-621.

9. Baroli I. et al. (2004) Photo-oxidative stress in a xanthophyll-deficient mutant of Chlamydomonas. *Journal of Biological Chemistry* **279**, 6337-6344.

10. Bechtold U., Karpinski S., & Mullineaux P.M. (2005) The influence of the light environment and photosynthesis on oxidative signalling responses in plant-biotrophic pathogen interactions. *Plant Cell and Environment* **28**, 1046-1055.

11. Berthold D., Babcock G., & Yocum C. (1981) A highly resolved, oxygen-evolving photosystem II preparation from spinach thylakoid membranes: EPR and electron-transport properties. *Febs Letters* **134**, 231-234.

12. Breyton C. et al. (2006) Redox Modulation of Cyclic Electron Flow around Photosystem I in C3 Plants. *Biochemistry* **45**, 13465-13475.

13. Bugos R.C., Chang S.H., & Yamamoto H. (1999) Developmental expression of violaxanthin de-epoxidase in leaves of tobacco growing under high and low light. *Plant Physiol* **121**, 207-214.

14. Chang C.C. et al. (2004) Induction of ASCORBATE PEROXIDASE 2 expression in wounded Arabidopsis leaves does not involve known wound-signalling pathways but is associated with changes in photosynthesis. *Plant J.* **38**, 499-511.

15. Chaves M.M., Maroco J.P., & Pereira J.S. (2003) Understanding plant responses to drought - from genes to the whole plant. *Functional Plant Biology (formerly Australian Journal of Plant Physiology)* **30**, 239-264.

16. Christmann A. et al. (2006) Integration of abscisic acid signalling into plant responses. *Plant Biology* **8**, 314-325.

17. Congming L. et al. (2003) PSII photochemistry, thermal energy dissipation, and the xanthophyll cycle in *Kalanchoä daigremontiana* exposed to a combination of water stress and high light. *Physiologia Plantarum* **118**, 173-182.

18. Cruz J.A. et al. (2005) Plasticity in light reactions of photosynthesis for energy production and photoprotection. *Journal of Experimental Botany* **56**, 395-406.

19. de Las Rivas J., Abadia A., & Abadia J. (1989) A New Reversed Phase-HPLC Method Resolving All Major Higher Plant Photosynthetic Pigments. *Plant Physiol* **91**, 190-192.

20. Demmig B. et al. (1987) Photoinhibition and Zeaxanthin Formation in Intact Leaves : A Possible Role of the Xanthophyll Cycle in the Dissipation of Excess Light Energy. *Plant Physiol* **84**, 218-224.

21. Demmig-Adams B. & Adams W.W. (2006a) Photoprotection in an ecological context: the remarkable complexity of thermal energy dissipation. *New Phytologist* **172**, 11-21.

22. Demmig-Adams B. et al. (2006) Modulation of PsbS and flexible vs sustained energy dissipation by light environment in different species. *Physiologia Plantarum* **127**, 670-680.

23. Ebbert V. et al. (2005) Up-regulation of a photosystem II core protein phosphatase inhibitor and sustained D1 phosphorylation in zeaxanthin-retaining, photoinhibited needles of overwintering Douglas fir. *Plant Cell and Environment* **28**, 232-240.

24. Egorova E.A. & Bukhov N.G. (2006) Mechanisms and functions of photosystem I-related alternative electron transport pathways in chloroplasts. *Russian Journal of Plant Physiology* **53**, 571-582.

25. Eskling M., Arvidsson P.-O., & Åkerlund H.-E. (1997) The xanthophyll cycle, its regulation and components. *Physiologia Plantarum* **100**, 806-816.

26. Foyer C.H. & Mullineaux P.M. (1998) The presence of dehydroascorbate and dehydroascorbate reductase in plant tissues. *FEBS Lett.* **425**, 528-529.

27. Foyer C.H., Lelandais M., & Kunert K.J. (1994) Photooxidative stress in plants. *Physiol Plant*.

28. Fryer M.J. et al. (2003) Control of Ascorbate Peroxidase 2 expression by hydrogen peroxide and leaf water status during excess light stress reveals a functional organisation of Arabidopsis leaves. *Plant J.* **33**, 691-705.

29. Fryer M.J. et al. (2002) Imaging of photo-oxidative stress responses in leaves. *J.Exp.Bot.* **53**, 1249-1254.

30. Garcia-Plazaola J.I. & Becerril J.M. (1999) A rapid high performance liquid chromatography method to measure lipophilic antioxidants in stressed plants: Simultaneous determination of carotenoids and tocopherols. *Phytochemical Analysis* **10**, 307-313.

31. Gechev T.S. et al. (2006) Reactive oxygen species as signals that modulate plant stress responses and programmed cell death. *BioEssays*.

32. Gechev T.S. & Hille J. (2005) Hydrogen peroxide as a signal controlling plant programmed cell death. *Journal of Cell Biology* **168**, 17-20.

33. Gilmore A.M. (1997b) Mechanistic aspects of xanthophyll cycle-dependent photoprotection in higher plant chloroplasts and leaves. *Physiologia Plantarum* **99**, 197-209.

34. Hideg E. et al. (2002) Detection of singlet oxygen and superoxide with fluorescent sensors in leaves under stress by photoinhibition or UV radiation. *Plant and Cell Physiology* **43**, 1154-1164.

35. Hieber A.D., Kawabata O., & YAMAMOTO H.Y. (2004) Significance of the lipid phase in the dynamics and functions of the xanthophyll cycle as revealed by PsbS overexpression in tobacco and in-vitro de-epoxidation in monogalactosyldiacylglycerol micelles. *Plant and Cell Physiology* **45**, 92-102.

36. Holt N.E., Fleming G.R., & Niyogi K.K. (2004) Toward an understanding of the mechanism of nonphotochemical quenching in green plants. *Biochemistry* **43**, 8281-8289.

37. Horton P. & Ruban A. (2005) Molecular design of the photosystem II light-harvesting antenna: photosynthesis and photoprotection. *Journal of Experimental Botany* **56**, 365-373.

38. Jain M. et al. (2006) Validation of housekeeping genes as internal control for studying gene expression in rice by quantitative real-time PCR. *Biochemical and Biophysical Research Communications* **345**, 646-651.

39. Kalituho L. et al. (2006) Characterization of a nonphotochemical quenching-deficient Arabidopsis mutant possessing an intact PsbS protein, xanthophyll cycle and lumen acidification. *Planta* **223**, 532-541.

40. Krieger-Liszkay A. (2005) Singlet oxygen production in photosynthesis. *J.Exp.Bot.* **56**, 337-346.

41. Kruk J. et al. (2005) Tocopherol as singlet oxygen scavenger in photosystem II. *J.Plant Physiol* **162**, 749-757.

42. Latowski D., Grzyb J., & Strzalka K. (2004) The xanthophyll cycle - molecular mechanism and physiological significance. *Acta Physiologiae Plantarum* **26**, 197-212.

43. Li X.P. et al. (2000) A pigment-binding protein essential for regulation of photosynthetic light harvesting. *Nature* **403**, 391-395.

44. Logan B.A. et al. (1999) Effect of nitrogen limitation on foliar antioxidants in relationship to other metabolic characteristics. *Planta* **209**, 213-220.

45. Long S.P., Humphries S., & Falkowski P.G. (1994) Photoinhibition of Photosynthesis in Nature. *Annual Review of Plant Physiology and Plant Molecular Biology* **45**, 633-662.

46. Ma Y.Z. et al. (2003) Evidence for direct carotenoid involvement in the regulation of photosynthetic light harvesting. *Proceedings of the National Academy of Sciences of the United States of America* **100**, 4377-4382.

47. Makino A., Miyake C., & Yokota A. (2002) Physiological functions of the water-water cycle (Mehler reaction) and the cyclic electron flow around PSI in rice leaves. *Plant and Cell Physiology* **43**, 1017-1026.

48. Maxwell K. & Johnson G.N. (2000) Chlorophyll fluorescence - a practical guide. *Journal of Experimental Botany* **51**, 659-668.

49. Meisel L. et al. (2005) A rapid and efficient method for purifying high quality total RNA from peaches (Prunus persica) for functional genomics analyses. *Biological Research* **38**, 83-88.

50. Mittler R. (2002) Oxidative stress, antioxidants and stress tolerance. *Trends Plant Sci.* **7**, 405-410.

51. Montillet J.L. et al. (2004) The upstream oxylipin profile of Arabidopsis thaliana: a tool to scan for oxidative stresses. *Plant J.* **40**, 439-451.

52. Muller M. et al. (2006) Enhanced alpha-tocopherol quinone levels and xanthophyll cycle de-epoxidation in rosemary plants exposed to water deficit during a Mediterranean winter. *Journal of Plant Physiology* **163**, 601-606.

53. Mullineaux P. & Karpinski S. (2002) Signal transduction in response to excess light: getting out of the chloroplast. *Curr.Opin.Plant Biol.* **5**, 43-48.

54. Mullineaux P.M., Karpinski S., & Baker N.R. (2006) Spatial dependence for hydrogen peroxide-directed signaling in light-stressed plants. *PLANT PHYSIOLOGY* **141**, 346-350.

55. Munne-Bosch S. & Alegre L. (2000) Changes in carotenoids, tocopherols and diterpenes during drought and recovery, and the biological significance of chlorophyll loss in Rosmarinus officinalis plants. *Planta* **210**, 925-931.

56. Munne-Bosch S. & Penuelas J. (2004) Drought-induced oxidative stress in strawberry tree (Arbutus unedo L.) growing in Mediterranean field conditions. *Plant Science* **166**, 1105-1110.

57. Nicot N. et al. (2005a) Housekeeping gene selection for real-time RT-PCR normalization in potato during biotic and abiotic stress. *Journal of Experimental Botany* **56**, 2907-2914.

58. Niyogi K.K. (1999) PHOTOPROTECTION REVISITED: Genetic and Molecular Approaches. *Annu.Rev.Plant Physiol Plant Mol.Biol.* **50**, 333-359.

59. Niyogi K.K. et al. (2005) Is PsbS the site of non-photochemical quenching in photosynthesis? *Journal of Experimental Botany* **56**, 375-382.

60. North H.M. et al. (2005) Analysis of xanthophyll cycle gene expression during the adaptation of Arabidopsis to excess light and drought stress: Changes in RNA steady-state levels do not contribute to short-term responses. *Plant Science* **169**, 115-124.

61. Ort D.R. & Baker N.R. (2002) A photoprotective role for O(2) as an alternative electron sink in photosynthesis? *Curr.Opin.Plant Biol.* **5**, 193-198.

62. Oxborough K. & Baker N.R. (1997) An instrument capable of imaging chlorophyll alpha fluorescence from intact leaves at very low irradiance and at cellular and subcellular levels of organization. *Plant Cell and Environment* **20**, 1473-1483.

63. Reddy A.R., Chaitanya K.V., & Vivekanandan M. (2004) Drought-induced responses of photosynthesis and antioxidant metabolism in higher plants. *Journal of Plant Physiology* **161**, 1189-1202.

64. Rizhsky L., Liang H., & Mittler R. (2003) The water-water cycle is essential for chloroplast protection in the absence of stress. *J.Biol.Chem.* **278**, 38921-38925..

65. Rossel J.B. et al. (2006) A mutation affecting ASCORBATE PEROXIDASE 2 gene expression reveals a link between responses to high light and drought tolerance. *Plant Cell and Environment* **29**, 269-281.

66. Rossel J.B., Wilson I.W., & Pogson B.J. (2002) Global changes in gene expression in response to high light in Arabidopsis. *Plant Physiol* **130**, 1109-1120.

67. Sambrook,J., Fritsch,E.F., & Maniatis,T. (1989) Molecular Cloning: a Laboratory Manual, p. 7.3-7.4. Cold Spring Harbor Laboratory Press, New York.

68. Thompson J.D., Higgins D.G., & Gibson T.J. (1994) Clustal-W - Improving the Sensitivity of Progressive Multiple Sequence Alignment Through Sequence Weighting, Position-Specific Gap Penalties and Weight Matrix Choice. *Nucleic Acids Research* **22**, 4673-4680.

69. Verhoeven A.S., Demmig-Adams B., & Adams III W.W. (1997) Enhanced Employment of the Xanthophyll Cycle and Thermal Energy Dissipation in Spinach Exposed to High Light and N Stress. *Plant Physiol* **113**, 817-824.

70. Woitsch S. & Romer S. (2003) Expression of xanthophyll biosynthetic genes during light-dependent chloroplast differentiation. *Plant Physiol* **132**, 1508-1517.